Chemico-Biological Interactions 345 (2021) 109555

Contents lists available at ScienceDirect

Chemico-Biological Interactions

journal homepage: www.elsevier.com/locate/chembioint

Research paper

Structure based design, synthesis, and evaluation of anti-CML activity of the quinolinequinones as LY83583 analogs

Nilüfer Bayrak [a], Halil I. Ciftci [b,c], Mahmut Yıldız [d], Hatice Yıldırım [a], Belgin Sever [c,e], Hiroshi Tateishi [c], Masami Otsuka [b,c], Mikako Fujita [c,**], Amaç Fatih Tuyun [f,*]

[a] Department of Chemistry, Faculty of Engineering, Istanbul University-Cerrahpasa, Avcilar, Istanbul, Turkey
[b] Department of Drug Discovery, Science Farm Ltd., Kumamoto, Japan
[c] Medicinal and Biological Chemistry Science Farm Joint Research Laboratory, School of Pharmacy, Kumamoto University, Kumamoto, Japan
[d] Chemistry Department, Gebze Technical University, Gebze, Kocaeli, Turkey
[e] Department of Pharmaceutical Chemistry, Faculty of Pharmacy, Anadolu University, Eskisehir, Turkey
[f] Department of Chemistry, Faculty of Science, Istanbul University, Fatih, Istanbul, Turkey

ARTICLE INFO

Keywords:
LY83583
Quinolinequinones
Aminoquinone
Apoptosis
Chronic myelogenous leukemia (CML)
DNA-Cleavage
Structure-activity relationship (SAR)

ABSTRACT

Quinone-based small molecules are the promising structures for antiproliferative drug design and can induce apoptosis in cancer cells. Among them, one of the quinolinequinones, named as 6-anilino-5,8-quinolinequinone, LY83583 has the ability to inhibit the growth of cancer cells as an inhibitor of cyclase. The biological potential of all synthesized compounds as the analogs of the identified lead molecule LY83583 that possessed the antiproliferative efficiency was determined. The two series of the LY83583 analogs containing electron-withdrawing or electron-donating group(s) were synthesized and subsequently *in vitro* evaluated for their cytotoxic activity against K562, Jurkat, MT-2, and HeLa cell lines using MTT assay. All the LY83583 analogs showed antiproliferative activity with good IC_{50} values (less than positive control imatinib). Four analogs from each series were also selected for the determination of selectivity against human peripheral blood mononuclear cells (PBMCs). The analog **AQQ15** showed high potency towards all cancer cell lines with almost similar selectivity of imatinib. In order to get a better insight into cytotoxic effects of the analog **AQQ15** in K562 cells, further apoptotic effects due to annexin V/ethidium homodimer III staining, ABL1 kinase inhibition, and DNA cleaving ability were examined. The analog **AQQ15** induced apoptotic cell death in K562 cells with 34.6% compared to imatinib (6.5%). This analog showed no considerable ABL1 kinase inhibitory activity but significant DNA cleavage activity indicating DNA fragmentation-induced apoptosis. Besides, molecular docking studies revealed that the analog **AQQ15** established proper interactions with the deoxyribose sugar attached with the nucleobases adenine and guanidine respectively, in the minor groove of the double helix of DNA. *In silico* predicted pharmacokinetic parameters of this analog were found to comply with the standard range making it an efficient anticancer drug candidate for further research.

1. Introduction

An immense number of natural products (generally defined as small-molecule secondary metabolites) serving as drugs for the treatment of many life-threatening diseases that exist in nature originating from plants, bacteria, fungi, and marine life forms and play a fundamental role in chemical biology [1–4]. In recent years, the use of natural products or natural product-like small molecules which enable the success of privileged structures is of both biological and medicinal interest [2,4]. The anthracyclines doxorubicin (Doxils; Adriamycins), daunorubicin (Cerubidines), and epirubicin (Ellences), for example, are typically well-known drugs used in cancer treatment [4,5]. Most of the clinically approved anticancer drugs in the market have been inspired by natural products which constitute a broad biodiversity of molecules [6,7].

Streptonigrin (**1**) shown in Fig. 1, a bioactive alkaloid, was first isolated from *Streptomyces flocculus* in 1959; afterwards, the following year (in 1960), the first member of quinolinequinones (QQs) was

* Corresponding author.
** Corresponding author.
E-mail addresses: mfujita@kumammot-u.ac.jp (M. Fujita), aftuyun@gmail.com, aftuyun@istanbul.edu.tr (A.F. Tuyun).

https://doi.org/10.1016/j.cbi.2021.109555
Received 25 March 2021; Received in revised form 22 May 2021; Accepted 10 June 2021
Available online 16 June 2021
0009-2797/© 2021 Elsevier B.V. All rights reserved.

originally introduced as an antitumor agent [8] against cancer cell lines [9,10] and an antiviral agent against viruses including HIV-1 [11–13]. The discovery of streptonigrin (**1**) in the 1970s for anticancer activity against leukemia cell lines attracted the attention of researchers [14]. In the human clinical phase (for oral and parenteral application), the studies showed that the streptonigrin (**1**) was found effective against malignant lymphomas, mycosis fungoides, and Hodgkin's disease [15]. Besides, the use of streptonigrin (**1**) was limited due to the toxicity, whereas it is still one of the most important templates for the design of new drugs in the future [16,17]. The researchers continued to find an ample ground between the therapeutic efficacy and reduced toxicity. As a next step, lavendamycin (**2**) [18,19] and streptonigron (**3**) [19,20], the structurally analogs of streptonigrin (**1**), were originally isolated from the *Streptomyces* species (Fig. 1). Recent evidences have suggested that a significant number of lavendamycin analogs have displayed strong anticancer activity with low animal toxicity [21,22]. Additionally, streptonigron (**3**) was also proposed for its high anticancer, antibacterial, and antiviral activities [14]. The structure-activity relationship (SAR) studies of QQs by Kremer (1967) pointed out that the replacement of carbonyl group with NH group led to a decrease in activity, as in azastreptonigrin (**4**) [23]. Thus, what we know about pharmaceutical activity for streptonigrin (**1**), lavendamycin (**2**), or streptonigron (**3**) are mainly based on *p*-quinone moiety [24]. Since the streptonigrin (**1**) is composed of four rings designated A (*p*-quinone), B (pyridine), C (substituted pyridine), and D (substituted phenyl), a considerable amount of literature has been published on examining the structures of the most potent compounds [25,26]. The extensive SAR studies on structural modification particularly conducted by Johnson [24] have revealed that the QQ moiety (AB ring system) has played a critical role in the anticancer potency [26–28]. In addition to this finding, rings C (pyridyl moiety) and D (the substituted phenyl moiety) are not essential for the activity in murine cancer cell lines, whereas these moieties have enhanced the anticancer activity against the human cancer cell lines [15,24]. Commercially available anticancer drug LY83583 (6-anilino-5, 8-quinolinequinone) outlined in Fig. 1, which acts also as an inhibitor of guanylyl cyclase, prevents cell proliferation in cancer cells that produced through over production of reactive oxygen species [29–31]. We have recently reported the discovery of Plastoquinone analogs (based on dimethyl amino-1,4-benzoquinones) that are responsible for their selective anticancer efficacy which induces the apoptosis in cancer cell leaving the normal cells safe [32–34]. In these works, SAR studies of the Plastoquinone analogs revealed that (a) the existence of the group(s) within the aminophenyl ring and (b) the presence of a chlorine atom were important. Taking into account the aforementioned data, in the present work, we have designed and synthesized new QQs for cancer drug research by further realization since LY83583 is used as the lead compound for the design. As shown in Fig. 1, the LY83583 structure consists of three fragments (aminophenyl, 1,4-quinonyl, and pyridyl moieties). Thus, we have decided to merge these important points from our recent reports with LY83583 both by replacing the methyl groups with a pyridyl ring (to form a QQ moiety) and inserting the different group(s) within the aminophenyl ring (Fig. 2). In addition to the design and synthesis of QQs, these two series of QQs were first evaluated *in vitro* against four cancer cell lines (K562 (myeloid leukemia), HeLa (human cervical carcinoma), Jurkat, and MT-2 (other two human T-cell leukemia)). Then, the most promising analogs were tested against human peripheral blood mononuclear cells (PBMCs) to determine the selectivity index (SI). The most selective and efficient anticancer agent towards K562 cells was further searched for its apoptotic effects based on Hoechst 33342/annexin V/ethidium homodimer III staining, ABL1 kinase inhibition, and DNA cleavage capacity. Molecular docking studies were also carried out for the analogs with the most significant DNA cleavage efficiency to detect its binding potential to DNA. *In silico* Absorption, Distribution, Metabolism, and Excretion (ADME) studies were also assessed for all synthesized analogs to understand the compliance of compounds with particular pharmacokinetic determinants.

2. Results and discussion

2.1. Design and chemical synthesis

The attention of our research group has long focused on the interactions of different types of 1,4-quinones as electron-deficient compounds with electron-rich reagents (nucleophiles), obtaining compounds with promising biological (antimicrobial and/or anticancer) activities [32–38]. The synthetic pathway of a series of LY83583 analogs substituted with different group(s) on aminophenyl ring is shown in Table 1. For the synthesis of a series of LY83583 analogs (QQs), following a literature procedure reported by Shaikh et al. [24], the starting compound (6,7-dichloro-5,8-quinolinequinone, **2**) was obtained by the oxidation of commercially available 8-hydroxyquinoline (**1**) with sodium chlorate in concentrated HCl solution. Within this field of research, a considerable amount of literature has been published on the reactions of QQs with different nucleophiles [39–43]. These data clearly indicate that QQs are very reactive towards nucleophiles such as thiols [41,44], amines [45,46], and alcohols [47,48]. The product distribution is highly sensitive to modification of the reaction conditions such as molar ratios of substrates, reagents, and polarity of reaction medium

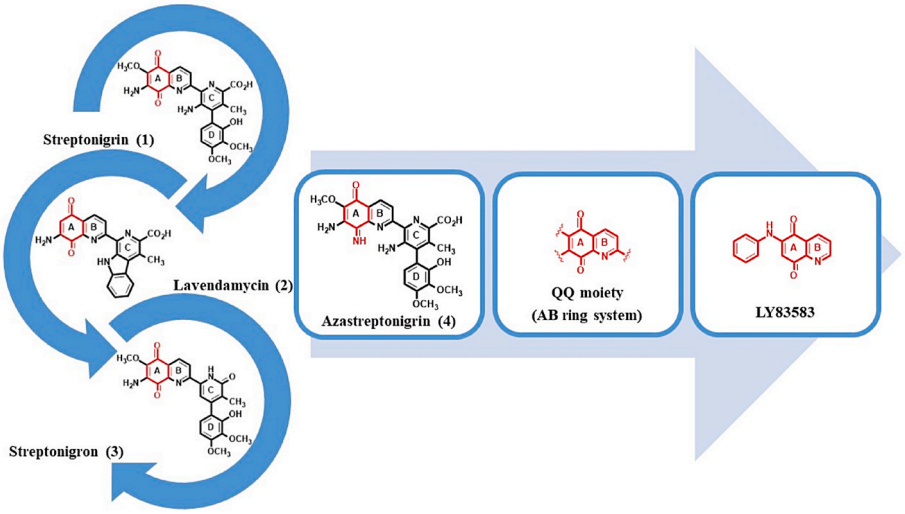

Fig. 1. Discovery of LY83583 based on QQ moiety starting from natural products.

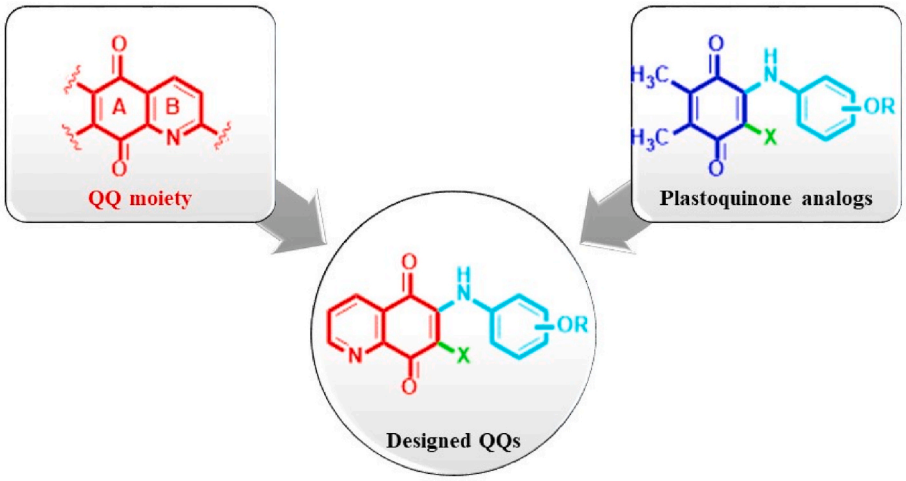

Fig. 2. Design of QQs.

Table 1
Preparation of two subseries (**AQQ1-19**) of the LY83583 as its analogs.

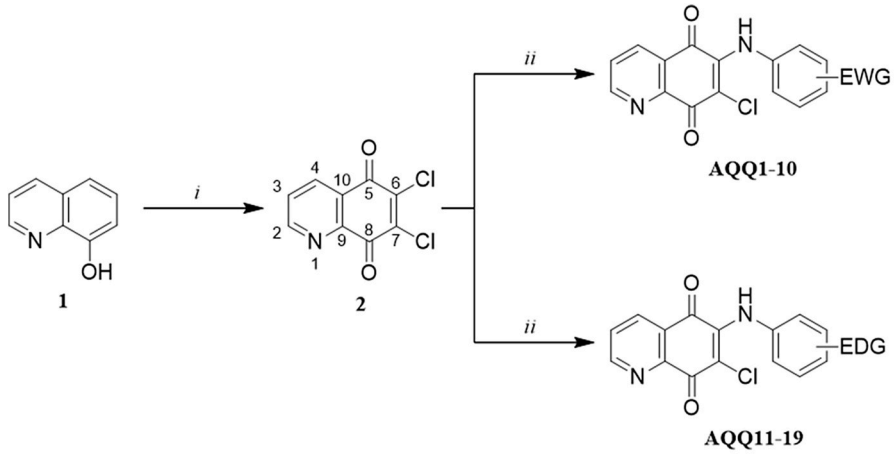

Reagents and conditions:
(*i*) $NaClO_3$, HCl, 50-60°C; (*ii*) $CeCl_3.7H_2O$, corresponding aryl amines, EtOH, rt to reflux, 3-6 h.
Arbitrary numbering is for convenience.

ID	EWG	ID	EWG	ID	EDG	ID	EDG
AQQ1	2-$COOCH_3$	**AQQ6**	4-$COOCH_2CH_3$	**AQQ11**	2,3-diCH_3 [55]	**AQQ16**	2-$CH(CH_3)_2$
AQQ2	3-$COOCH_3$	**AQQ7**	2-$COOC(CH_3)_3$	**AQQ12**	2,4-diCH_3	**AQQ17**	3-$CH(CH_3)_2$
AQQ3	4-$COOCH_3$	**AQQ8**	3-$COOC(CH_3)_3$	**AQQ13**	2,5-diCH_3	**AQQ18**	4-$CH(CH_3)_2$
AQQ4	2-$COOCH_2CH_3$	**AQQ9**	4-$COOC(CH_3)_3$	**AQQ14**	3,4-diCH_3 [53]	**AQQ19**	4-$N(CH_2CH_3)_2$
AQQ5	3-$COOCH_2CH_3$	**AQQ10**	4-CN	**AQQ15**	3,5-diCH_3		

[14,49,50]. First of all, discussing QQs' nucleophilic reactivity, it must be remarked that the two chlorine atoms are not equivalent in it and that mostly one linked at C-6 and/or C-7 is "selectively" substituted by amines depending on the reaction medium and/or reagents [51,52]. The chemistry and SAR of the C-6 and/or C-7 substituted QQs are the major research areas of previous reports. Therefore, the substituents linked at C-6 and/or C-7 are mainly versatile groups such as amino, ether, and thioether, as well as nitro, alkyl, and halogen groups. Furthermore, previous studies from other groups have also proved that C-6 substituted QQs have a very significant effect on bioactivity [43,45]. In the literature concerning the product distribution, the presence of the Lewis acids such as $NiCl_2.6H_2O$ [45] or $CeCl_3.7H_2O$ [53] as a catalyst in a reaction media promotes the substitution with the chlorine atom linked at C-6 since the electron density of C-6 is reduced *via* the chelation of Ce(III) between nitrogen atom in B ring and oxygen atom linked at C-8 as depicted in Fig. 3 [50,54]. Besides, polar solvents like water or ethanol are also known to increase the formation of C-6 substituted QQs [50].

The regioselective insertion of aromatic amines was conducted into the corresponding C-6 substituted QQs (a series of LY83583 analogs) by nucleophilic substitution of aromatic amines to electrophilic 1,4-quinone according to the procedure under Ce(III) catalysis (Table 1) [53]. For the synthesis of the first subseries of a series of LY83583 analogs, **AQQ1-10** was obtained by the amination reaction of 6, 7-dichloro-5,8-quinolinequinone (**2**) in the presence of $CeCl_3.7H_2O$ with aryl amines containing electron-withdrawing groups (EWGs) such as ester and cyano groups (-COOR and –CN) at different positions. The second subseries of the target analogs (a series of LY83583 analogs) were synthesized in the same method. The reaction of 6,7-dichloro-5, 8-quinolinequinone (**2**) with aryl amines containing electron-donating groups (EDGs) such as alkyl and amino groups (-R and $–NR_2$) at

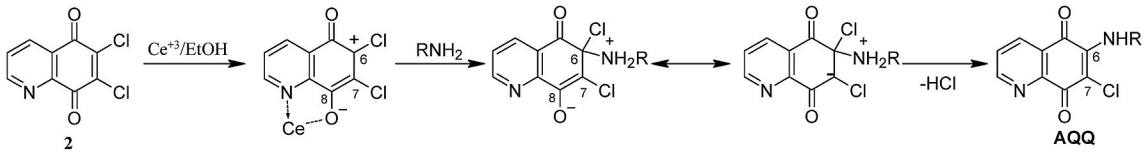

Fig. 3. Preferential nucleophilic substitution with the addition of $CeCl_3.7H_2O$ at C-6.

different positions in ethanol resulted in other LY83583 analogs (**AQQ11**–**19**). After the synthesis and purification, the structures of a series of LY83583 analogs were evaluated by using diverse modern analytical techniques like Fourier-transform infrared spectroscopy (FTIR), ^{1}H nuclear magnetic resonance (NMR), ^{13}C NMR, and high-resolution mass spectrometry (HRMS).

2.2. Crystal structures

X-ray crystallographic studies have also shown that the nucleophilic substitution actually has taken place at C-6 or C-7 [43,53]. The representative molecular structures of **AQQ3**, **AQQ7**, **AQQ13**, and **AQQ15** have been characterized by single crystal X-ray crystallography technique to verify both structural skeleton of presented novel products and the regioselectivity of the substitution reaction as described in the experimental section. The ORTEP diagrams are depicted in Fig. 4. The target analogs (**AQQ3**, **AQQ7**, **AQQ13**, and **AQQ15**) were dissolved in ethanol and kept for crystallization to afford good quality diffraction crystal for one week.

AQQ3 and **AQQ7** crystallize in the monoclinic crystal system (space group *Cc and P 1* 21*/c 1,* respectively), **AQQ13** crystallizes in a triclinic crystal system (space group P1), and **AQQ15** crystallizes in an orthorhombic crystal system (space group Ibca) as shown in Table 2. The ORTEP drawings of the **AQQ3**, **AQQ7**, **AQQ13**, and **AQQ15** were reported at a 50% probability level in Fig. 4. The crystallographic data of these analogs indicate that the C–O bond lengths of the carbonyl groups marked as C6–O1 and C9–O2 are, on average, 1.218 Å. This value is compatible with the carbonyl group (C═O) bond length of the quinolinequinones [43]. When the ester groups attached to the benzene ring of **AQQ3** and **AQQ7** are examined; the C═O double bond lengths are 1.199 Å and 1.218 Å, while the C–O single bond lengths between the carbonyl carbon and alkoxide oxygen are 1.329 Å and 1.327 Å, respectively. The difference between these two C–O bond lengths supports that there is not any resonance form. The esters having a carbonyl center gives to 120° C–C–O and O–C–O bond angles due to sp^2 hybridization. In accordance with this situation; O3–C16–O4 and O3–C16–C15 bond angles of **AQQ7** are 124.0° and 123.9°; O4–C16–O3 and C13–C16–O4 bond angles of **AQQ3** are 122.3° and 124.6°, respectively. The C–O–C bond angle of the ester group is 116.1° for **AQQ3**, and 123.3° for **AQQ7**. One reason for the different bond angles is that **AQQ3** has a methyl group in the ester group, whereas in **AQQ7** the ester group contains *tert*-butyl. As known, the *tert*-butyl group is bulkier than the methyl group. Therefore, the steric effect of *tert*-butyl results that a larger bond angle of the C–O–C bond. In terms of bond distances and angles, the molecular geometry of **AQQ** derivatives is compatible with the expected data. The details of all crystallographic data of **AQQ3, AQQ7, AQQ13**, and **AQQ15** are summarized in the Supplementary file.

2.3. Biological evaluation

The antiproliferative activity of the LY83583 analogs (**AQQ1-19**) was investigated *in vitro* against K562 (myeloid leukemia), Jurkat, MT-2 (other two human T-cell leukemia) cell lines, and HeLa (human cervical carcinoma) cell line as summarized in Table 3 by employing 3-(4,5-dimethylthiazol-2-yl)-2,5-diphenyltetrazolium bromide (MTT) assay. Imatinib was used as a positive control. We used imatinib as a positive control because it has been proven to specifically inhibit ABL, which is expressed in nearly all cases of and has increased the overall survival of patients with CML from 4 years to an estimated 19–25 years [56–58]. The inhibitory concentrations that completed 50% inhibition (IC_{50}) of cancer cell growth of all analogs are listed in Table 3. Having better antileukemia activity in the K562 cell line (suspension cells) in our previous studies [32–34], we added the HeLa cell line (adherent cells) for the determination of the further antiproliferative activity of the analogs. Results indicated that some analogs (**AQQ2**, **AQQ3**, **AQQ5**, **AQQ7**, **AQQ14**, **AQQ15**, **AQQ18**, and **AQQ19**) showed better antiproliferative activity against leukemia cells than HeLa cells (Table 3). These analogs were also found as more effective anti-leukemic agents against K562 and Jurkat cells than MT-2 cells. The analogs (**AQQ2**, **AQQ14**, **AQQ15**, **AQQ18**, and **AQQ19**) demonstrated the most robust antiproliferative activity towards the K562 cell line with the IC_{50} values of 1.27 ± 0.16 μM, 0.74 ± 0.08 μM, 0.52 ± 0.06 μM, 0.62 ± 0.07 μM, and 0.67 ± 0.04 μM, respectively when compared with imatinib (IC_{50} = 5.71 ± 1.02 μM). In a similar manner, the three analogs (**AQQ3**, **AQQ5**,

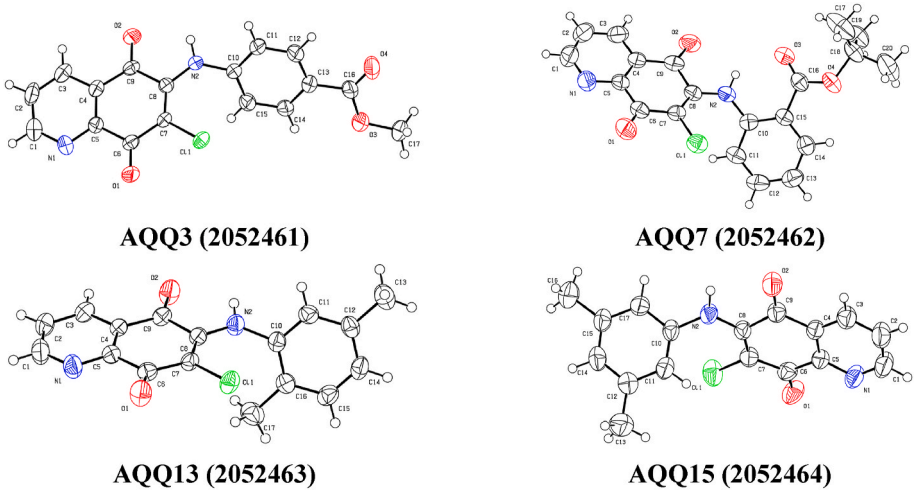

Fig. 4. ORTEP drawings of **AQQ3**, **AQQ7**, **AQQ13**, and **AQQ15** at 50% probability level.

Table 2
Crystallographic data for the LY83583 analogs (**AQQ3**, **AQQ7**, **AQQ13**, and **AQQ15**).

ID Code	AQQ3	AQQ7	AQQ13	AQQ15
Chemical formula	$C_{17}H_{11}ClN_2O_4$	$C_{20}H_{17}ClN_2O_4$	$C_{17}H_{13}ClN_2O_2$	$C_{17}H_{13}ClN_2O_2$
Formula weight (g mol^{-1})	342.74	384.80	312.74	312.74
Crystal system, space group/Z	Monoclinic, *Cc*/4	Monoclinic, P 1 21/c 1/2	Triclinic, P-1	Orthorhombic, Ibca/16
Temperature (K)	273.15	296(2)	296(2)	273(2)
Wavelength (Å)	0.71073	0.71073	0.71073	0.71073
a, b, c (Å)	*a* = 4.6642 (12) *b* = 27.835 (7) *c* = 11.840 (3)	*a* = 17.579(13) *b* = 13.345(10) *c* = 8.074(6)	*a* = 8.1605(14) *b* = 9.3384(15) *c* = 10.5442(17)	*a* = 13.98(2) *b* = 16.39(2) *c* = 25.48(4)
α, β, γ (°)	β = 98.088 (4) α, γ = 90	β = 98.042(13) α, γ = 90	α = 76.593(2) β = 67.276(2) γ = 81.824(3)	α, β, γ = 90
V ($Å^3$)	1521.9 (7)	1875.(2)	719.7(2)	5838.(14)
Crystal sizes (mm^3)	0.27 × 0.14 × 0.11	0.04 × 0.07 × 0.41	0.06 × 0.09 × 0.25	0.05 × 0.08 × 0.20
D_{cal} (g cm^{-3})	1.496	1.363	1.443	1.423
Absorption coefficient, μ (mm^{-1})	0.280	0.232	0.274	0.270
Goodness-of-fit on F^2	0.894	1.006	1.042	1.012

Table 3
General Formula and Cytotoxicity of LY83583 Analogs (**AQQ1-19**) in K562, Jurkat, MT-2, and HeLa Cell Lines for 24 h.

LY83583 Analogs		Subseries (X)	Substituent(s)	Cell Type (IC_{50}, μM)[a]				SI[d]	SI[e]
General Formula	ID			K562[b]	Jurkat[b]	MT-2[b]	HeLa[b]		
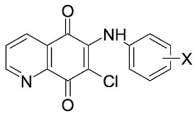 **X = EWG or EDG**	**AQQ1**	EWG	2-$COOCH_3$	2.13 ± 0.38	1.64 ± 0.22	2.57 ± 0.18	8.25 ± 2.36	0.77	3.87
	AQQ2		3-$COOCH_3$	1.27 ± 0.16	1.45 ± 0.25	2.78 ± 0.34	6.51 ± 1.22	1.14	5.13
	AQQ3		4-$COOCH_3$	1.87 ± 0.27	1.44 ± 0.31	2.74 ± 0.25	7.86 ± 1.47	0.77	4.20
	AQQ4		2-$COOCH_2CH_3$	2.18 ± 0.27	1.47 ± 0.18	2.92 ± 0.33	7.61 ± 1.64	0.67	3.49
	AQQ5		3-$COOCH_2CH_3$	1.48 ± 0.13	1.29 ± 0.30	2.86 ± 0.26	7.76 ± 2.54	0.87	5.24
	AQQ6		4-$COOCH_2CH_3$	2.40 ± 0.13	1.57 ± 0.36	2.70 ± 0.16	8.88 ± 1.58	0.65	3.67
	AQQ7		2-$COOC(CH_3)_3$	1.71 ± 0.22	1.53 ± 0.42	2.66 ± 0.42	7.91 ± 1.08	0.89	4.63
	AQQ8		3-$COOC(CH_3)_3$	2.67 ± 0.46	1.86 ± 0.39	3.81 ± 0.53	8.17 ± 1.74	0.70	3.06
	AQQ9		4-$COOC(CH_3)_3$	2.76 ± 0.27	1.61 ± 0.27	2.35 ± 0.44	9.01 ± 2.15	0.58	3.26
	AQQ10		4-CN	2.98 ± 0.51	1.27 ± 0.24	3.38 ± 0.45	9.05 ± 2.93	0.43	3.04
	AQQ11	EDG	2,3-diCH_3	2.48 ± 0.45	2.11 ± 0.35	5.44 ± 0.66	6.43 ± 1.20	0.85	2.59
	AQQ12		2,4-diCH_3	1.99 ± 0.27	2.02 ± 0.15	8.44 ± 1.54	3.78 ± 0.51	1.02	1.90
	AQQ13		2,5-diCH_3	1.65 ± 0.32	1.57 ± 0.17	5.13 ± 0.97	2.57 ± 0.23	0.95	1.56
	AQQ14		3,4-diCH_3	0.74 ± 0.08	1.35 ± 0.14	5.58 ± 0.72	6.62 ± 0.84	1.82	8.95
	AQQ15		3,5-diCH_3	0.52 ± 0.06	0.78 ± 0.07	3.13 ± 0.35	2.77 ± 0.31	1.50	5.33
	AQQ16		2-$CH(CH_3)_2$	1.68 ± 0.23	2.00 ± 0.36	3.92 ± 0.50	3.90 ± 0.61	1.19	2.32
	AQQ17		3-$CH(CH_3)_2$	1.73 ± 0.19	1.46 ± 0.28	4.39 ± 0.83	6.68 ± 0.95	0.84	3.86
	AQQ18		4-$CH(CH_3)_2$	0.62 ± 0.07	0.74 ± 0.09	2.14 ± 0.49	6.86 ± 1.15	1.19	11.06
	AQQ19		4-$N(CH_2CH_3)_2$	0.67 ± 0.04	1.30 ± 0.16	2.77 ± 0.56	5.39 ± 1.34	1.94	8.04
	Imatinib[c]			5.71 ± 1.02	6.45 ± 1.34	13.27 ± 5.15	16.35 ± 4.96	1.13	2.86

[a] The reported values represent the mean ± SD for each analog based on three independent experiments.
[b] Cell lines include myeloid leukemia (K562), other two human T-cell leukemia (Jurkat and MT-2), and human cervical carcinoma (HeLa).
[c] Used as the positive control.
[d] SI = IC_{50} for Jurkat cell line/IC_{50} for K562 cell line.
[e] SI = IC_{50} for HeLa cell line/IC_{50} for K562 cell line.

and **AQQ7**) exhibited the lowest IC_{50} values (1.44 ± 0.31 μM, 1.29 ± 0.30 μM, and 1.53 ± 0.42 μM, respectively) towards Jurkat cells as compared to imatinib (IC_{50} = 6.45 ± 1.34 μM) (Table 3).

LY83583 analogs were designed to analyze the SARs using synthetic analogs in order to clarify the crucial functional group(s) and its position in the aminophenyl moiety for the antiproliferative activity as two series possessing an EWG or EDG group in the aminophenyl moiety to assess the importance of substituents. Collectively, the present two series of LY83583 analogs displayed a range of potencies against the four tested cancer cell lines. Among them, the analogs (**AQQ15** and **AQQ18**) exhibited high potency against K562 and Jurkat cell lines, with IC_{50} value less than 1 μM (Table 3). Notably, **AQQ15** displayed the most prominent growth inhibitory activities against these four cell lines with IC_{50} values ranging from 0.5 to 3.2 μM. In the case of Jurkat cells, all analogs (except **AQQ11**, **AQQ12**, and **AQQ16**) exhibited better antiproliferative activity than imatinib with IC_{50} value less than 2 μM. The analog (**AAQ13**) exhibited the strongest activity (IC_{50} ranging from 2.5 to 4.0 μM) followed by the analog (**AAQ15**) against the HeLa cell line. These results suggested that these two series of LY83583 analogs could effectively suppress cancer growth since all of the tested LY83583 analogs showed better cytotoxicity than the positive control (imatinib) against all tested cancer cell lines.

In order to evaluate the selectivity of the most active LY83583 analogs (**AQQ2**, **AQQ3**, **AQQ5**, **AQQ7**, **AQQ14**, **AQQ15**, **AQQ18**, and **AQQ19**), we examined their cytotoxic effects on PBMCs and calculated the SI (Table 4) by dividing the IC_{50} of the PBMC growth inhibition with the K562 cell growth inhibition for each. Amongst them, the analog (**AQQ15**) deserved special importance, because **AQQ15**, presenting the most favorable selectivity between PBMCs and K562 cells with a 4.06 SI value. Besides, the SI, which was calculated between Jurkat and K562 cells, was found as 1.50 for **AQQ15** showing its high selective anti-leukemic effects against K562 cells. Based on the aforementioned findings, **AQQ15** was subsequently selected for further mechanism research for providing deep insights into its notable anti-leukemic effects against K562 cells (Table 4).

Based on the biological data obtained so far, SAR correlations were

Table 4
The cytotoxicity of selected LY83583 analogs and selectivity.

LY83583 Analogs		Subseries (X)	Substituent(s)	Cell Type (IC_{50}, μM)		SI[b]
General Formula	ID			K562[a]	PBMC[a]	
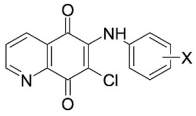 X = EWG or EDG	**AQQ2**	EWG	3-$COOCH_3$	1.27 ± 0.16	1.58 ± 0.18	1.24
	AQQ3		4-$COOCH_3$	1.87 ± 0.27	3.78 ± 0.25	2.02
	AQQ5		3-$COOCH_2CH_3$	1.48 ± 0.13	3.39 ± 0.52	2.29
	AQQ7		2-$COOC(CH_3)_3$	1.71 ± 0.22	1.52 ± 0.21	0.89
	AQQ14	EDG	3,4-diCH_3	0.74 ± 0.08	2.69 ± 0.27	3.64
	AQQ15		3,5-diCH_3	0.52 ± 0.06	2.11 ± 0.16	4.06
	AQQ18		4-$CH(CH_3)_2$	0.62 ± 0.07	0.97 ± 0.13	1.56
	AQQ19		4-$N(CH_2CH_3)_2$	0.67 ± 0.04	0.90 ± 0.08	1.34
	Imatinib[c]			5.71 ± 1.02	27.14 ± 5.37	4.75

[a] Cell lines include myeloid leukemia (K562) and peripheral blood mononuclear cells (PBMC).
[b] The selectivity index (SI) values are calculated by dividing the IC_{50} of the PBMC growth inhibition with the K562 cell growth inhibition.
[c] Used as the positive control.

analyzed. Firstly, we evaluated the effects of the EWG group within the LY83583 analogs on the cytotoxic activity. Generally, with the changing the alkyl moiety in the ester group (from methyl to *tert*-butyl) at the *para* position, the cytotoxic activities decreased in the obtained analogs against K562, Jurkat, and HeLa cell lines. The alteration of the position of the ester group displayed no any remarkable change in the activity against any cancer cell line. On the other hand, the replacement of the ester group with the cyano group at the *para* position in the first subseries did not show any significant effect. Regarding the second subseries, the target analogs with EDG were more potent than the analogs containing EWG. The analogs with an alkyl group(s) as an EDG group at the *para* position showed relatively higher potency. The analog (**AQQ15**) led to a considerable increase in potency against K562 and Jurkat cell lines. The use of isopropyl or diethylamino with substitution at *para* position for target analogs (**AQQ18** and **AQQ19**) clearly indicated that these donor groups improved the activity compared to the ester group.

Based on the promising MTT results of the analog **AQQ15**, initially apoptotic effects of this analog in the K562 cell line were investigated compared to imatinib using Hoechst 33342/annexin V/ethidium homodimer III staining assay monitored by fluorescence microscope (Fig. 5a). This method expresses the difference between necrosis and apoptosis related to the staining with ethidium homodimer III (red) and annexin V (green), respectively. The analog **AQQ15** was detected to have a substantial influence on apoptotic cell death in K562 cells with 34.6% compared to imatinib (6.5%). Moreover, it can be deduced that the analog **AQQ15** was more effective (6.7%) than imatinib (3.6%) at the late apoptotic/necrotic phase of the K562 cell line (Fig. 5b, Table 5). These observations accentuated that in CML cells, the analog **AQQ15** underwent apoptosis, an important pathway for cancer prevention [59].

The BCR-ABL1 tyrosine kinase has been reported to constitute an attractive target for CML therapy related to its critical roles in the survival and proliferation of CML cells. However, the role of ABL1 tyrosine kinase in the regulation of apoptosis has remained unlightened so far due to the fusion of the c-*abl* gene with the *bcr* gene in the formation of BCR-ABL1 hybrid protein making confusion about the exact biological functions of ABL1 kinase [60].

In this work, based on the aforementioned data, how the ABL1 kinase inhibitory activity of the analog **AQQ15** contributed to the apoptosis in the K562 cells compared to imatinib was subsequently speculated. As depicted in Fig. 6 and Table 6, the analog **AQQ15** showed no considerable ABL1 kinase inhibitory activity as compared to imatinib at 1 μM and 10 μM concentrations implying that the analog **AQQ15** induced apoptosis in K562 cells without inhibiting ABL1 kinase.

Oligonucleosomal DNA degradation and chromatin condensation attract great attention in the apoptotic program. Furthermore, the discovery of DNA cleavage during apoptosis with the evidence of discrete ladder (apoptosis) of bands instead of smear (necrosis) also changed the beliefs about the only digestion of the cells to death and release of proteases [61].

Subsequent mechanism including the relationship between DNA cleavage potency and apoptosis induction was explored using the electrophoresis in agarose gel. This method explains the three distinct patterns of plasmid DNA entitled Form I (supercoiled), Form II (single break), and Form III (double break or linear form) [62]. Results suggested that the analog **AQQ15** exerted its apoptotic functions by disrupting pUC 19 DNA. Of note, the analog **AQQ15** was found to possess the capacity to cleave DNA in the presence and absence of $FeSO_4$, H_2O_2, and ascorbic acid. Ultimately, the analog **AQQ15** exhibited augmented DNA-cleaving activity with 41% intensity of Form II band and 4% intensity of Form III band (Fig. 7c) within the iron (II) complex system after 40 min (Figs. 7a) and 60 min (Fig. 7b).

2.4. Molecular docking and ADME prediction

After confirming that the analog **AQQ15** was able to cleave DNA significantly, we next turned our attention to assessing molecular docking study to warrant the experimental data of biological experiments conjecturing the binding orientation of the analog **AQQ15** with DNA. In accordance with this purpose, the crystal structure of DNA was retrieved from the Protein Data Bank server (PDB entry: 1BNA) [62,63]. The analog **AQQ15** exhibited significantly higher binding affinity to DNA with corresponding π-π stacking interactions with DA-17 and DG-16 *via* its quinoline and 3,5-dimethyl phenyl moieties, respectively in the minor groove of the double helix of DNA. However, the analog **AQQ15** also established a hydrogen bonding with DA-18, which led to a reduction in its strong binding capacity to DNA (Fig. 8a and b).

A number of crucial physicochemical properties of the analogs **AQQ1-19** such as predicted aqueous solubility (QPlogS), human serum albumin binding (QPlogKhsa), predicted octanol/water partition coefficient (QPlogPo/w), predicted human oral absorption, compatibility with Lipinski's rule of 5 and Jorgensen's rule of 3 were in silico postulated. The results were found coherent with acceptable ranges of all these specified parameters (Table 7). These properties were particularly were preferred due to their substantial direct or indirect effects in membrane permeability, tissue penetration, metabolism, clearance, bioavailability, and toxicity of drugs. The analogs of LY83583 (**AQQ1-19**) displayed notable QPlogS and QPlogPo/w values ranging from (−5.55 to −3.75) and (1.76–3.75), respectively, which were within the acceptable ranges in order (−6.5 to 0.5) and (−2 to 6.5). The QPlogKhsa values of all analogs (−0.32 to 0.31) were also determined at the appropriate range (−1.5 to 1.5). Moreover, the analogs of LY83583 (**AQQ1-19**) presented significant human oral absorption (79.91–100%) on a 0–100% scale (>80% is high; <25% is poor) and no violation of Lipinski's and Jorgensen's parameters [64,65].

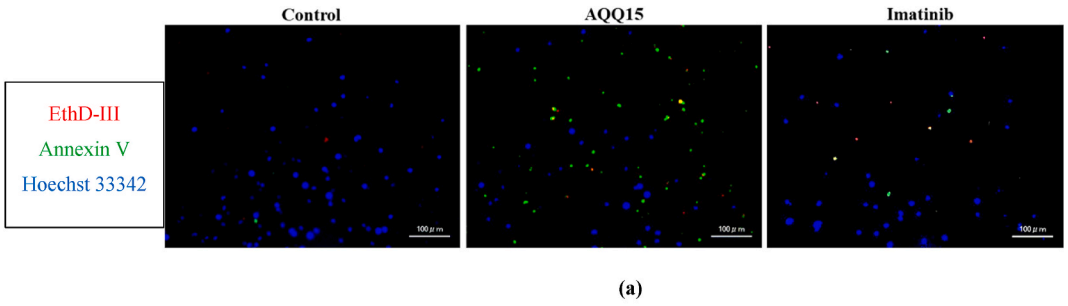

(a)

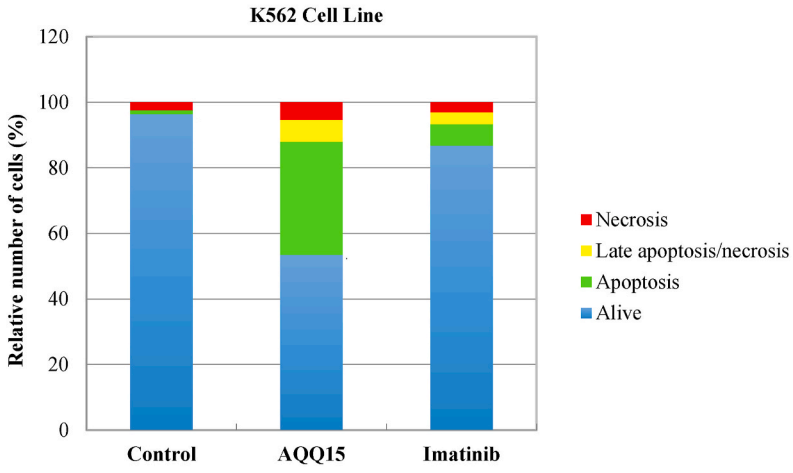

(b)

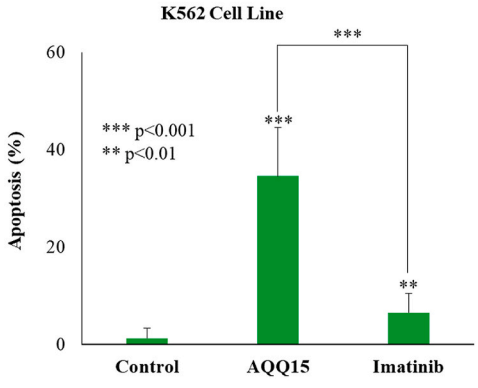

(c)

Fig. 5. Changes in K562 cell line at 1 μM concentration of control, **AQQ15** and imatinib for 12 h **(a)**. A total of approximately 1000 stained cells were selected randomly in each experiment of **(a)** and were classified as 4 groups, namely, "alive" (blue), "apoptosis" (green), "necrosis or late apoptosis" (yellow) and "necrosis" (red) **(b)**. Quantification of the effect of the analog **AQQ15** and imatinib on apoptosis. Data from three independent experiments are shown as means ± standard deviations and p values were determined using Student's test **(c)**.

Table 5
The percentage of apoptotic cells treated with the analog **AQQ15** and Imatinib.

Compound	K562 cell line			
	Alive	Apoptosis%	Late Apoptosis/Necrosis%	Necrosis%
Control	96.4	1.2	0.0	2.4
AQQ15	53.4	34.6	6.7	5.3
Imatinib	86.8	6.5	3.6	3.1

3. Conclusion

In our continuing investigations of 1,4-quinones, two subseries of the LY83583 analogs (**AAQ1-19**) were designed and synthesized. Enthused by the biological significance of QQs, the 1,4-quinone and aminophenyl moieties are retained in target analogs, but the 1,4-quinone moiety has been extended by the addition of a pyridine moiety, in order to increase the activity. As per the results obtained from *in vitro* antiproliferative evaluation, the analog (**AAQ15**) was identified as the most potent analog with the highest growth inhibition against the K562 cell line and acceptable SI value compared with the positive control. This analog further induced apoptosis in the K562 cell line associated with its

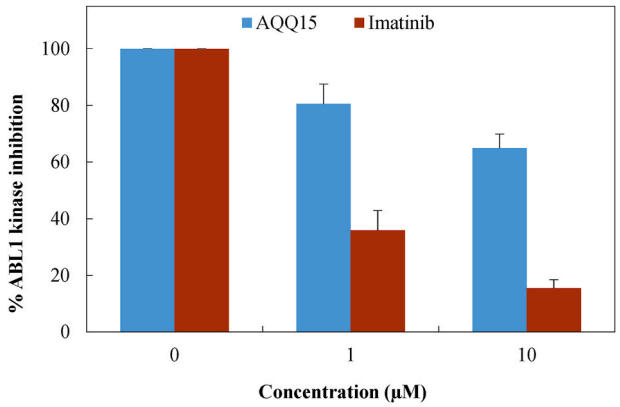

Fig. 6. The ABL1 kinase inhibition of the analog **AQQ15** and Imatinib at 1 μM and 10 μM concentrations.

Table 6
The ABL1 kinase inhibition of the analog **AQQ15** and Imatinib.

Concentration (μM)	Relative Activity (%)	
	AQQ15	Imatinib
1	19.4	64.1
10	35.1	84.6

significant DNA cleavage potential. In addition, the above results provide a useful correlation between the original natural streptonigrin (**1**), described in Fig. 1, and **AQQ15** in DNA cleavage activity and confirm that QQ moiety (AB ring system) is the responsible part for activity [24, 66]. Molecular docking studies also accentuated that the analog **AAQ15** formed important π-π stacking interactions in the minor groove of the double helix of DNA. Furthermore, results of in silico ADME studies revealed that the analog **AAQ15** was found coherent with all the ranges of specified crucial pharmacokinetic determinants suggesting that this analog possessed anticancer drug-like properties for future studies.

4. Experimental section

4.1. Chemistry

Melting points (Mp) were determined with a Buchi B-540 melting point apparatus and are uncorrected. All reagents were commercially obtained from a commercial suppliers and used without further purification unless specified otherwise. Thin layer chromatography (TLC) was conducted on Merck KGaA (silica gel 60 F254) based on Merck DC-plates (aluminum based). Compound visualization for TLC during the chromatographic separation was accomplished by UV irradiation at 254 nm. Chromatography refers to column chromatography performed on silica gel 60 (Merck, 63–200 μm particle sized, 60–230 mesh) with eluent. FTIR spectra were recorded on a PerkinElmer Spectrum 100 Optical FTIR spectrometer by applying ATR Sampling Accessory for both oil and solid compounds. HRMS was performed on either a Waters SYNAPT G1 MS or an Agilent 6530 Accurate-MassQ-TOF LC/MS. Mass spectra were obtained on a BRUKER Microflex LT by MALDI (Matrix Assisted Laser Desorption Ionization)-TOF technique *via* addition of 1,8,9-anthracenetriol (DIT, dithranol) as matrix. Proton and carbon NMR spectra were recorded at 500 MHz/125 MHz (^{1}H NMR/^{13}C NMR) on Varian^{UNITY} INOVA spectrometers in parts per million (ppm, δ). ^{1}H NMR spectra and ^{13}C NMR spectra in $CDCl_3$ and DMSO-d_6 refer to the solvent signal center. Coupling constants (J) were reported in Hz. Standard abbreviations indicating multiplicity were used as follows: *s* (singlet), *br s* (broad singlet), *d* (doublet), *t* (triplet), *m* (multiplet), and *dd* (doublet of doublets). Data for the single crystal compounds were obtained with Bruker APEX II QUAZAR three-circle diffractometer. Indexing was performed using APEX2 [67]. Data integration and reduction were carried out with SAINT [68]. Absorption correction was performed by multi-scan method implemented in SADABS [69]. The Bruker SHELXTL [70] software package was used for structures solution and structure refinement. Aromatic C-bound and N-bound hydrogen atoms were positioned geometrically and refined using a riding mode. Crystal structure validations and geometrical calculations were performed using the Platon software [71]. Mercury software [72] was used for visualization of the. cif files. 6,7-Dichloro-5,8-quinolinequinone (**2**) was synthesized using the reported method by Shaikh et al. [24] in the literature.

4.2. Procedure for the synthesis of the quinolinequinone (2) [24]

6,7-Dichloro-5,8-quinolinequinone (**2**) was prepared according to the literature from 8-hydroxyquinoline and sodium chlorate in concentrated HCl in 29% yield. Mp 219–220 °C (Lit [24]. 221–223 °C). ^{1}H NMR (500 MHz, *CDCl$_3$*) δ (ppm): 9.40 (d, J = 4.39 Hz, 1H, $CH_{aromatic}$), 8.44–8.48 (m, 1H, $CH_{aromatic}$), 7.67–7.72 (m, 1H, $CH_{aromatic}$). ^{13}C NMR (125 MHz, *CDCl$_3$*) δ (ppm): 174.6, 173.3 (>C═O), 154.4, 145.8, 143.4, 142.1, 134.6, 127.3, 127.2 ($C_{aromatic}$ and C_q). MS (+ESI) *m/z* (%): 248 (100, $[M + Na–2H]^+$), 250 (93, $[M+Na]^+$); Anal. Calcd. for $C_9H_3Cl_2NO_2$ (226.95).

4.3. General procedure for the synthesis of the amino substituted quinolinequinones (AQQ1-19) [53]

A suspension of the **2** (0.285 g, 1.25 mmol) and $CeCl_3.7H_2O$ (0.512 g, 1.375 mmol, 1.1 equiv) in ethanol was stirred at room temperature for 1 h. Then, a suspension of the corresponding amines (1.375 mmol, 1.1 equiv) in ethanol was added to that solution and refluxed for 3–6 h until consumption of the **2**. The reaction mixture was cooled to room temperature. After evaporation of the solvent, the residue was dissolved with CH_2Cl_2 (50 mL), and the solution was washed sequentially with water (3 x 30 mL). The organic layer was dried over anhydrous $CaCl_2$, filtered, and concentrated under reduced pressure, and the residue was purified by means of column chromatography on silica gel to give the corresponding **AQQ**.

4.3.1. Methyl 2-((7-chloro-5,8-dioxo-5,8-dihydroquinolin-6-yl)amino) benzoate (AQQ1)

By subjecting the mixture (**2** and $CeCl_3.7H_2O$) and methyl 2-aminobenzoate (0.208 g, 1.375 mmol) to the general procedure for the synthesis of the **AQQ1**, the title compound (**AQQ1**) was purified by column chromatography as a dark red solid. Yield: 33%, mp 250–251 °C. FTIR (ATR) υ (cm^{-1}): 3248 (NH), 3052 ($CH_{aromatic}$), 2988, 2915 ($CH_{aliphatic}$), 1687, 1672 (>C═O), 1590, 1558, 1506, 1457, 1363, 1321, 1251, 1228, 1142, 1088, 1058, 1021. ^{1}H NMR (500 MHz, *CDCl$_3$*) δ (ppm): 10.18 (s, 1H, $CH_{aromatic}$), 9.09 (s, 1H, $CH_{aromatic}$), 8.49 (d, J = 7.7 Hz, 1H, $CH_{aromatic}$), 8.04 (d, J = 7.7 Hz, 1H, $CH_{aromatic}$), 7.75–7.60 (m, 1H, NH), 7.60–7.45 (m, 1H, $CH_{aromatic}$), 7.18 (t, J = 7.6 Hz, 1H, $CH_{aromatic}$), 6.86 (d, J = 8.2 Hz, 1H, $CH_{aromatic}$), 3.99 (s, 3H, OCH_3). ^{13}C NMR (125 MHz, *CDCl$_3$*) δ (ppm): 179.77, 175.83, 167.86 (>C═O), 155.20, 148.00, 140.66, 138.97, 135.07, 132.40, 130.96, 127.41, 127.22, 123.25, 123.06, 119.71, 118.83 ($C_{aromatic}$ and C_q), 52.51 (OCH_3). HRMS(+ESI) *m/z* calcd for $C_{17}H_{12}^{35}ClN_2O_4$ $[M + H]^+$: 343.0486; found: 343.0486 and $C_{17}H_{12}^{37}ClN_2O_4$ $[M + H]^+$: 345.0456; found: 345.0464.

4.3.2. Methyl 3-((7-chloro-5,8-dioxo-5,8-dihydroquinolin-6-yl)amino) benzoate (AQQ2)

By subjecting the mixture (**2** and $CeCl_3.7H_2O$) and methyl 3-aminobenzoate (0.208 g, 1.375 mmol) to the general procedure for the synthesis of the **AQQ2**, the title compound (**AQQ2**) was purified by column chromatography as a light brown solid. Yield: 55%, mp 197–198 °C. FTIR (ATR) υ (cm^{-1}): 3343 (NH), 3081 ($CH_{aromatic}$), 2956 ($CH_{aliphatic}$), 1716, 1670 (>C═O), 1610, 1576, 1501, 1439, 1295, 1214, 1146, 1102, 1064. ^{1}H NMR (500 MHz, *CDCl$_3$*) δ (ppm): 9.07 (s, 1H, $CH_{aromatic}$), 8.45

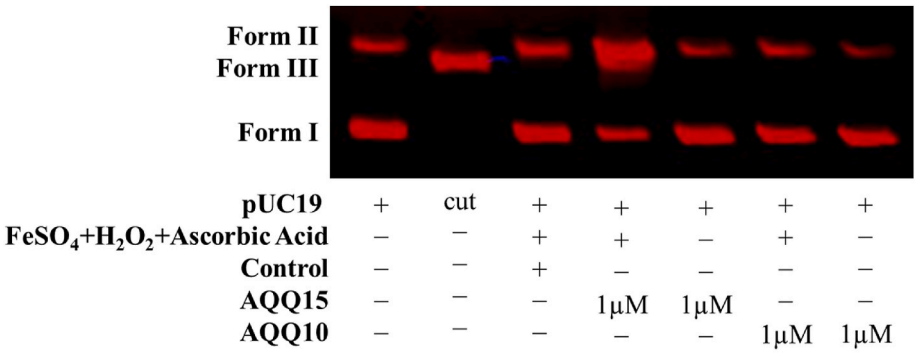

a

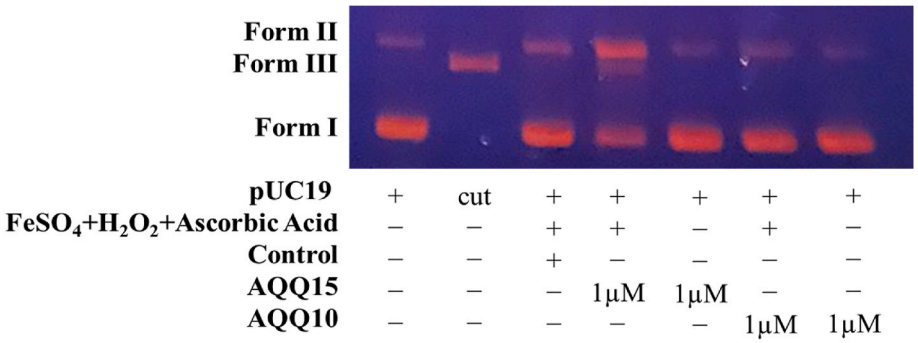

b

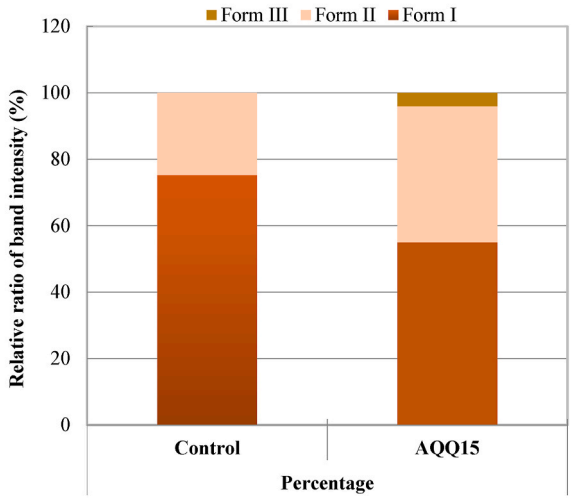

c

Fig. 7. The DNA-cleaving activity of **AQQ15** in the presence of $FeSO_4$, H_2O_2, and ascorbic acid system after 40 min (**a**) after 60 min (**b**). Relative intensity of form I, form II and form III bands.

(d, $J = 7.8$ Hz, 1H, $CH_{aromatic}$), 7.91 (d, $J = 7.7$ Hz, 1H, $CH_{aromatic}$), 7.76 (s, 1H, $CH_{aromatic}$), 7.72 (s, 1H, NH), 7.70–7.65 (m, 1H, $CH_{aromatic}$), 7.46 (t, $J = 7.8$ Hz, 1H, $CH_{aromatic}$), 7.28–7.30 (m, 1H, $CH_{aromatic}$), 3.93 (s, 3H, OCH_3).^{13}C NMR (125 MHz, *CDCl3*) δ (ppm): 179.89, 175.79, 166.22 (>C═O), 155.44, 148.21, 140.91, 137.36, 134.87, 130.70, 128.60, 128.42, 127.06, 126.95, 126.93, 125.06, 116.92 ($C_{aromatic}$ and C_q), 52.39 (OCH_3). HRMS(+ESI) *m/z* calcd for $C_{17}H_{12}^{35}ClN_2O_4$ $[M + H]^+$: 343.0486; found: 343.0487 and $C_{17}H_{12}^{37}ClN_2O_4$ $[M + H]^+$: 345.0456; found: 345.0471.

4.3.3. *Methyl 4-((7-chloro-5,8-dioxo-5,8-dihydroquinolin-6-yl)amino) benzoate (AQQ3)*

By subjecting the mixture (**2** and $CeCl_3.7H_2O$) and methyl 4-amino-benzoate (0.208 g, 1.375 mmol) to the general procedure for the synthesis of the **AQQ3**, the title compound (**AQQ3**) was purified by column chromatography as a red solid. Yield: 68%, mp 256–258 °C. FTIR (ATR)

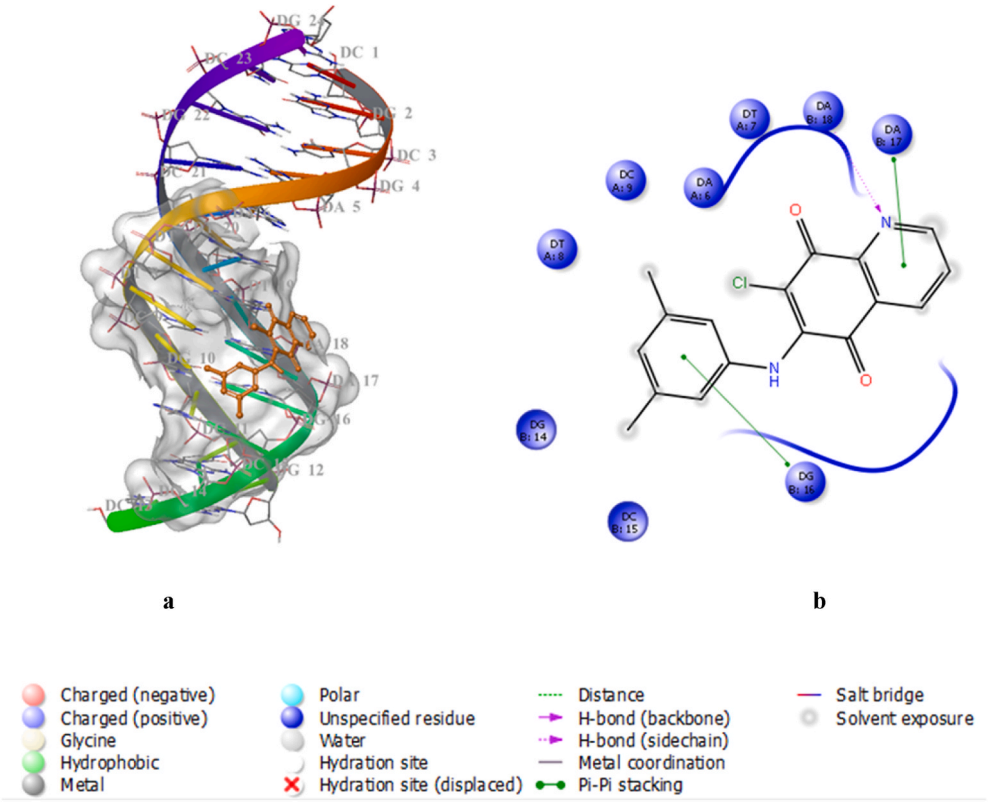

Fig. 8. Docking pose (**a**) and interactions (**b**) of the analog **AQQ15** (The ligand is highlighted in the orange colored stick) in the minor groove of the double helix of DNA (PDB code: 1BNA).

Table 7
Some ADME features of the analog of LY83583 (**AQQ1-19**).

The Analog	QPlogS[a]	QPlogPo/w[a]	QPlogKhsa[a]	Human Oral Absorption%	Rule of Five[a]	Rule of Three[b]
AQQ1	−3.75	2.57	−0.32	92.06	0	0
AQQ2	−4.07	2.50	−0.21	88.22	0	0
AQQ3	−4.09	2.49	−0.21	88.01	0	0
AQQ4	−4.27	2.88	−0.17	94.16	0	0
AQQ5	−4.63	2.80	0.02	90.43	0	0
AQQ6	−4.66	2.80	0.02	90.22	0	0
AQQ7	−5.05	3.63	0.25	96.33	0	0
AQQ8	−5.53	3.55	0.16	91.24	0	0
AQQ9	−5.55	3.54	0.17	91.23	0	0
AQQ10	−4.37	1.76	−0.25	93.87	0	0
AQQ11	−4.35	3.25	0.17	79.91	0	0
AQQ12	−4.68	3.28	0.10	100	0	0
AQQ13	−4.48	3.28	0.19	100	0	0
AQQ14	−4.59	3.26	0.19	95.81	0	0
AQQ15	−4.61	3.30	0.22	96.82	0	0
AQQ16	−4.58	3.57	0.26	100	0	0
AQQ17	−4.86	3.75	0.30	100	0	0
AQQ18	−4.88	3.72	0.31	100	0	0
AQQ19	−4.96	3.63	0.14	100	0	0

[a] **Rule of Five:** Number of violations of Lipinski's rule of five. The rules are: mol_MW (Molecular weight of the molecule) < 500, QPlogPo/w (Predicted octanol/water partition coefficient) < 5, donorHB (hydrogen-bond donor atoms) ≤ 5, accptHB (hydrogen-bond acceptor atoms) ≤ 10. Compounds that provide these rules are considered drug-like. (The "five" refers to the limits, which are multiples of 5).

[b] **Rule of Three:** Number of violations of Jorgensen's rule of three. The three rules are: QPlogS (Predicted aqueous solubility) > −5.7, QPPCaco (Predicted apparent Caco-2 cell permeability in nm/s) > 22 nm/s, # Primary Metabolites < 7. Compounds with fewer (and preferably no) violations of these rules are more likely to be orally available agents (Schrödinger Release 2016-2: Schrödinger, LLC, New York, NY, USA).

υ (cm^{-1}): 3207 (NH), 3093 ($CH_{aromatic}$), 2993 ($CH_{aliphatic}$), 1711, 1678 (>C═O), 1655, 1596, 1564, 1518, 1411, 1277, 1219, 1195, 1169, 1149, 1145, 1102, 1064. ^{1}H NMR (500 MHz, *CDCl₃*) δ (ppm): 9.10 (s, 1H, $CH_{aromatic}$), 8.48 (d, J = 7.9 Hz, 1H, $CH_{aromatic}$), 8.07 (d, J = 8.4 Hz, 2H, $CH_{aromatic}$), 7.77–7.58 (m, 2H, NH and $CH_{aromatic}$), 7.11 (d, J = 8.4 Hz, 2H, $CH_{aromatic}$), 3.95 (s, 3H, OCH_3).^{13}C NMR (125 MHz, *CDCl₃*) δ (ppm): 179.89, 175.79, 166.30 (>C═O), 155.52, 148.15, 141.08, 140.48, 134.92, 130.12, 127.18, 127.00, 126.93, 122.90 ($C_{aromatic}$ and C_q), 52.20 (OCH_3). HRMS(+ESI) *m/z* calcd for $C_{17}H_{12}^{35}ClN_2O_4$ [M + H]$^+$: 343.0486; found: 343.0485 and $C_{17}H_{12}^{37}ClN_2O_4$ [M + H]$^+$: 345.0456;

found: 345.0474.

4.3.4. Ethyl 2-((7-chloro-5,8-dioxo-5,8-dihydroquinolin-6-yl)amino) benzoate (AQQ4)

By subjecting the mixture (**2** and $CeCl_3.7H_2O$) and ethyl 2-aminobenzoate (0.227 g, 1.375 mmol) to the general procedure for the synthesis of the **AQQ4**, the title compound (**AQQ4**) was purified by column chromatography as a dark purple solid. Yield: 79%, mp 206–207 °C. FTIR (ATR) υ (cm^{-1}): 3255 (NH), 3081 ($CH_{aromatic}$), 2963, 2922 ($CH_{aliphatic}$), 1690, 1665 (>C═O), 1605, 1560, 1509, 1453, 1435, 1315, 1296, 1246, 1226, 1139, 1086, 1021. ^{1}H NMR (500 MHz, *CDCl$_3$*) δ (ppm): 10.21 (s, 1H, $CH_{aromatic}$), 9.08 (s, 1H, $CH_{aromatic}$), 8.49 (d, J = 7.8 Hz, 1H, $CH_{aromatic}$), 8.05 (d, J = 7.8 Hz, 1H, $CH_{aromatic}$), 7.68–7.70 (m, 1H, NH), 7.52 (d, J = 7.7 Hz, 1H, $CH_{aromatic}$), 7.17 (t, J = 7.7 Hz, 1H, $CH_{aromatic}$), 6.85 (d, J = 7.8 Hz, 1H, $CH_{aromatic}$), 4.45 (q, J = 7.1 Hz, 2H, OCH_2), 1.46 (t, J = 7.1 Hz, 3H, CH_3). ^{13}C NMR (125 MHz, *CDCl$_3$*) δ (ppm): 179.80, 175.84, 167.41 (>C═O), 155.18, 148.04, 140.66, 138.90, 135.03, 132.25, 130.97, 127.40, 127.18, 123.23, 123.04, 119.57, 119.18 ($C_{aromatic}$ and C_q), 61.61 (OCH_2), 14.25 (CH_3). HRMS(+ESI) *m/z* calcd for $C_{18}H_{14}^{35}ClN_2O_4$ $[M + H]^+$: 357.0642; found: 357.0641 and $C_{18}H_{14}^{37}ClN_2O_4$ $[M + H]^+$: 359.0613; found: 359.0632.

4.3.5. Ethyl 3-((7-chloro-5,8-dioxo-5,8-dihydroquinolin-6-yl)amino) benzoate (AQQ5)

By subjecting the mixture (**2** and $CeCl_3.7H_2O$) and ethyl 3-aminobenzoate (0.227 g, 1.375 mmol) to the general procedure for the synthesis of the **AQQ5**, the title compound (**AQQ5**) was purified by column chromatography as an orange solid. Yield: 74%, mp 152–154 °C. FTIR (ATR) υ (cm^{-1}): 3332 (NH), 3093 ($CH_{aromatic}$), 2981, 2933, 2907 ($CH_{aliphatic}$), 1721, 1664 (>C═O), 1600, 1578, 1568, 1506, 1444, 1363, 1287, 1272, 1211, 1184, 1138, 1103, 1067, 1032. ^{1}H NMR (500 MHz, *CDCl$_3$*) δ (ppm): 9.05 (s, 1H, $CH_{aromatic}$), 8.43 (s, 1H, $CH_{aromatic}$), 7.89 (s, 1H, $CH_{aromatic}$), 7.76 (s, 2H, $CH_{aromatic}$), 7.66 (s, 1H, NH), 7.43 (s, 1H, $CH_{aromatic}$), 7.27 (s, 1H, $CH_{aromatic}$), 4.49–4.21 (m, 2H, OCH_2), 1.47–1.26 (m, 3H, CH_3). ^{13}C NMR (125 MHz, *CDCl$_3$*) δ (ppm): 179.88, 175.76, 165.72 (>C═O), 155.44, 148.18, 140.96, 137.34, 134.90, 131.05, 128.50, 128.43, 127.10, 126.94, 126.91, 125.04, 116.78 ($C_{aromatic}$ and C_q), 61.34 (OCH_2), 14.30 (CH_3). HRMS(+ESI) *m/z* calcd for $C_{18}H_{14}^{35}ClN_2O_4$ $[M + H]^+$: 357.0642; found: 357.0639 and $C_{18}H_{14}^{37}ClN_2O_4$ $[M + H]^+$: 359.0613; found: 359.0593.

4.3.6. Ethyl 4-((7-chloro-5,8-dioxo-5,8-dihydroquinolin-6-yl)amino) benzoate (AQQ6)

By subjecting the mixture (**2** and $CeCl_3.7H_2O$) and ethyl 4-aminobenzoate (0.227 g, 1.375 mmol) to the general procedure for the synthesis of the **AQQ6**, the title compound (**AQQ6**) was purified by column chromatography as a red solid. Yield: 91%, mp 226–227 °C. FTIR (ATR) υ (cm^{-1}): 3212 (NH), 3089 ($CH_{aromatic}$), 2984 ($CH_{aliphatic}$), 1703, 1677 (>C═O), 1656, 1594, 1562, 1515, 1498, 1411, 1372, 1296, 1275, 1217, 1170, 1139, 1101, 1064, 1024. ^{1}H NMR (500 MHz, *CDCl$_3$*) δ (ppm): 9.08 (s, 1H, $CH_{aromatic}$), 8.46 (d, J = 7.7 Hz, 1H, $CH_{aromatic}$), 8.05 (d, J = 7.9 Hz, 2H, $CH_{aromatic}$), 7.75 (s, 1H, $CH_{aromatic}$), 7.69 (s, 1H, NH), 7.10 (d, J = 7.9 Hz, 2H, $CH_{aromatic}$), 4.39 (dd, J = 13.8, 6.8 Hz, 2H, OCH_2), 1.41 (t, J = 7.0 Hz, 3H, CH_3). ^{13}C NMR (125 MHz, *CDCl$_3$*) δ (ppm): 179.88, 175.79, 165.83 (>C═O), 155.51, 148.14, 140.99, 140.52, 134.91, 130.06, 127.29, 127.18, 126.99, 122.91, 118.29 ($C_{aromatic}$ and C_q), 61.11 (OCH_2), 14.35 (CH_3). HRMS(+ESI) *m/z* calcd for $C_{18}H_{14}^{35}ClN_2O_4$ $[M + H]^+$: 357.0642; found: 357.0637 and $C_{18}H_{14}^{37}ClN_2O_4$ $[M + H]^+$: 359.0613; found: 359.0621.

4.3.7. tert-Butyl 2-((7-chloro-5,8-dioxo-5,8-dihydroquinolin-6-yl)amino) benzoate (AQQ7)

By subjecting the mixture (**2** and $CeCl_3.7H_2O$) and *tert*-butyl 2-aminobenzoate (0.266 g, 1.375 mmol) to the general procedure for the synthesis of the **AQQ7**, the title compound (**AQQ7**) was purified by column chromatography as an orange solid. Yield: 13%, mp 153–154 °C. FTIR (ATR) υ (cm^{-1}): 3269 (NH), 3048 ($CH_{aromatic}$), 2970, 2930 ($CH_{aliphatic}$), 1697, 1681 (>C═O), 1607, 1594, 1567, 1510, 1449, 1367, 1296, 1269, 1221, 1160, 1144, 1083, 1019. ^{1}H NMR (500 MHz, *CDCl$_3$*) δ (ppm): 10.27 (s, 1H, $CH_{aromatic}$), 9.12 (s, 1H, $CH_{aromatic}$), 8.62–8.43 (m, 1H, $CH_{aromatic}$), 8.07–7.92 (m, 1H, $CH_{aromatic}$), 7.78–7.64 (m, 1H, NH), 7.63–7.42 (m, 1H, $CH_{aromatic}$), 7.23–7.12 (m, 1H, $CH_{aromatic}$), 6.93–6.74 (m, 1H, $CH_{aromatic}$), 1.65 (s, 9H, CH_3). ^{13}C NMR (125 MHz, *CDCl$_3$*) δ (ppm): 179.96, 175.84, 166.77 (>C═O), 155.17, 148.11, 140.68, 138.63, 135.11, 131.76, 131.18, 127.42, 127.16, 123.14, 123.06, 120.65, 119.36 ($C_{aromatic}$ and C_q), 82.69 (OC), 28.24 (CH_3). HRMS (+ESI) *m/z* calcd for $C_{20}H_{18}^{35}ClN_2O_4$ $[M + H]^+$: 385.0955; found: 385.0955 and $C_{20}H_{18}^{37}ClN_2O_4$ $[M + H]^+$: 387.0926; found: 387.0944.

4.3.8. tert-Butyl 3-((7-chloro-5,8-dioxo-5,8-dihydroquinolin-6-yl)amino) benzoate (AQQ8)

By subjecting the mixture (**2** and $CeCl_3.7H_2O$) and *tert*-butyl 3-aminobenzoate (0.266 g, 1.375 mmol) to the general procedure for the synthesis of the **AQQ8**, the title compound (**AQQ8**) was purified by column chromatography as a red solid. Yield: 83%, mp 162–163 °C. FTIR (ATR) υ (cm^{-1}): 3304 (NH), 3035 ($CH_{aromatic}$), 2970 ($CH_{aliphatic}$), 1707, 1675 (>C═O), 1656, 1592, 1563, 1508, 1432, 1370, 1299, 1158, 1111. ^{1}H NMR (500 MHz, *CDCl$_3$*) δ (ppm): 9.13 (s, 1H, $CH_{aromatic}$), 8.50 (s, 1H, $CH_{aromatic}$), 7.88 (s, 1H, $CH_{aromatic}$), 7.74 (s, 2H, NH and $CH_{aromatic}$), 7.69 (s, 2H, $CH_{aromatic}$), 7.45 (s, 1H, $CH_{aromatic}$), 1.62 (s, 9H, CH_3). ^{13}C NMR (125 MHz, *CDCl$_3$*) δ (ppm): 179.95, 175.77, 164.80 (>C═O), 148.31, 141.06, 137.10, 135.15, 132.71, 128.41, 128.35, 126.94, 125.04, 116.88 ($C_{aromatic}$ and C_q), 81.66 (OC), 28.18 (CH_3). HRMS(+ESI) *m/z* calcd for $C_{20}H_{18}^{35}ClN_2O_4$ $[M + H]^+$: 385.0955; found: 385.0955 and $C_{20}H_{18}^{37}ClN_2O_4$ $[M + H]^+$: 387.0926; found: 387.0948.

4.3.9. tert-Butyl 4-((7-chloro-5,8-dioxo-5,8-dihydroquinolin-6-yl)amino) benzoate (AQQ9)

By subjecting the mixture (**2** and $CeCl_3.7H_2O$) and *tert*-butyl 4-aminobenzoate (0.266 g, 1.375 mmol) to the general procedure for the synthesis of the **AQQ9**, the title compound (**AQQ9**) was purified by column chromatography as a red solid. Yield: 76%, mp 332–334 °C. FTIR (ATR) υ (cm^{-1}): 3244 (NH), 3100 ($CH_{aromatic}$), 2981 ($CH_{aliphatic}$), 1699, 1683 (>C═O), 1660, 1592, 1568, 1525, 1408, 1368, 1290, 1260, 1215, 1157, 1102. ^{1}H NMR (500 MHz, *CDCl$_3$*) δ (ppm): 9.08 (s, 1H, $CH_{aromatic}$), 8.46 (d, J = 7.7 Hz, 1H, $CH_{aromatic}$), 8.00 (d, J = 8.1 Hz, 2H, $CH_{aromatic}$), 7.77–7.56 (m, 2H, NH and $CH_{aromatic}$), 7.08 (d, J = 8.1 Hz, 2H, $CH_{aromatic}$), 1.61 (s, 9H, CH_3). ^{13}C NMR (125 MHz, *CDCl$_3$*) δ (ppm): 179.90 175.78, 164.96 (>C═O), 155.47, 148.16, 140.62, 140.58, 134.90, 129.89, 128.90, 127.13, 126.99, 122.89, 118.03 ($C_{aromatic}$ and C_q), 81.26 (OC), 28.19 (CH_3). HRMS(+ESI) *m/z* calcd for $C_{20}H_{18}^{35}ClN_2O_4$ $[M + H]^+$: 385.0955; found: 385.0955 and $C_{20}H_{18}^{37}ClN_2O_4$ $[M + H]^+$: 387.0926; found: 387.0953.

4.3.10. 7-Chloro-6-(4-cyanophenyl)amino-5,8-quinolinequinone (AQQ10)

By subjecting the mixture (**2** and $CeCl_3.7H_2O$) and 4-aminobenzonitrile (0.162 g, 1.375 mmol) to the general procedure for the synthesis of the **AQQ10**, the title compound (**AQQ10**) was purified by column chromatography as a red solid. Yield: 11%, mp 261–262 °C. FTIR (ATR) υ (cm^{-1}): 3341 (NH), 3070 ($CH_{aromatic}$), 2956, 2922, 2853 ($CH_{aliphatic}$), 2224 (CN), 1732, 1672, 1660 (>C═O), 1592, 1563, 1507, 1491, 1459, 1413, 1291, 1252, 1219, 1169, 1141. ^{1}H NMR (500 MHz, DMSO-d_6) δ (ppm): 9.63 (s, 1H, $CH_{aromatic}$), 9.01 (s, 1H, $CH_{aromatic}$), 8.40 (dd, J = 7.8 and 1.7 Hz, 1H, $CH_{aromatic}$), 7.82 (dd, J = 7.8 and 4.9 Hz, 1H, $CH_{aromatic}$), 7.74 (d, J = 8.7 Hz, 2H, $CH_{aromatic}$), 7.23 (d, J = 8.7 Hz, 2H, $CH_{aromatic}$). ^{13}C NMR (125 MHz, DMSO-d_6) δ (ppm): 180.19, 176.14 (>C═O), 154.81, 147.99, 144.30, 142.45, 134.94, 132.76, 128.46, 128.03, 122.63, 121.68, 119.66 ($C_{aromatic}$ and C_q), 105.05 (CN). HRMS(+ESI) *m/z* calcd for $C_{16}H_9ClN_3O_2$ $[M + H]^+$: 310.0383; found: 310.0379.

4.3.11. 7-Chloro-6-(2,3-dimethylphenyl)amino-5,8-quinolinequinone (AQQ11) [55]

By subjecting the mixture (**2** and $CeCl_3.7H_2O$) and 2,3-dimethylaniline (0.167 g, 1.375 mmol) to the general procedure for the synthesis of the **AQQ11**, the title compound (**AQQ11**) was purified by column chromatography as an orange solid. Yield: 22%, mp 197–198 °C. FTIR (ATR) υ (cm^{-1}): 3327 (NH), 3089 ($CH_{aromatic}$), 2921, 2856 ($CH_{aliphatic}$), 1664 (>C═O), 1608, 1579, 1568, 1497, 1460, 1310, 1269, 1220, 1138, 1077. ^{1}H NMR (500 MHz, DMSO-d_6) δ (ppm): 9.12 (s, 1H, $CH_{aromatic}$), 8.98 (s, 1H, $CH_{aromatic}$), 8.38 (d, J = 7.5 Hz, 1H, $CH_{aromatic}$), 7.96–7.65 (m, 1H, NH), 7.32–6.88 (m, 3H, $CH_{aromatic}$), 2.28 (s, 3H, CH_3), 2.12 (s, 3H, CH_3). ^{13}C NMR (125 MHz, DMSO-d_6) δ (ppm): 180.19, 175.56 (>C═O), 154.92, 148.29, 144.33, 138.17, 137.06, 134.84, 133.65, 128.46, 127.75, 127.54, 125.44, 125.22, 112.70 ($C_{aromatic}$ and C_q), 20.48, 14.84 (CH_3). HRMS(+ESI) *m/z* calcd for $C_{17}H_{14}^{35}ClN_2O_2$ [M + H]$^+$: 313.0744; found: 313.0741 and $C_{17}H_{14}^{37}ClN_2O_2$ [M + H]$^+$: 315.0714; found: 315.0727.

4.3.12. 7-Chloro-6-(2,4-dimethylphenyl)amino-5,8-quinolinequinone (AQQ12)

By subjecting the mixture (**2** and $CeCl_3.7H_2O$) and 2,4-dimethylaniline (0.167 g, 1.375 mmol) to the general procedure for the synthesis of the **AQQ12**, the title compound (**AQQ12**) was purified by column chromatography as an orange solid. Yield: 79%, mp 191–192 °C. FTIR (ATR) υ (cm^{-1}): 3328 (NH), 3085 ($CH_{aromatic}$), 2915, 2856 ($CH_{aliphatic}$), 1664 (>C═O), 1605, 1578, 1568, 1508, 1483, 1461, 1308, 1263, 1216, 1139, 1121. ^{1}H NMR (500 MHz, *CDCl$_3$*) δ (ppm): 9.12–9.01 (m, 1H, $CH_{aromatic}$), 8.51–8.37 (m, 1H, $CH_{aromatic}$), 7.74–7.59 (m, 1H, $CH_{aromatic}$), 7.53–7.42 (m, 1H, NH), 7.14–6.89 (m, 3H, $CH_{aromatic}$), 2.37 (s, 3H, CH_3), 2.27 (s, 3H, CH_3). ^{13}C NMR (125 MHz, *CDCl$_3$*) δ (ppm): 180.08, 175.69 (>C═O), 155.38, 148.46, 141.93, 137.21, 134.75, 133.77, 133.35, 131.12, 131.06, 126.82, 126.61, 126.33, 114.44 ($C_{aromatic}$ and C_q), 21.04, 18.11 (CH_3). HRMS(+ESI) *m/z* calcd for $C_{17}H_{14}^{35}ClN_2O_2$ [M + H]$^+$: 313.0744; found: 313.0740 and $C_{17}H_{14}^{37}ClN_2O_2$ [M + H]$^+$: 315.0714; found: 315.0738.

4.3.13. 7-Chloro-6-(2,5-dimethylphenyl)amino-5,8-quinolinequinone (AQQ13)

By subjecting the mixture (**2** and $CeCl_3.7H_2O$) and 2,5-dimethylaniline (0.167 g, 1.375 mmol) to the general procedure for the synthesis of the **AQQ13**, the title compound (**AQQ13**) was purified by column chromatography as a red solid. Yield: 32%, mp 175–176 °C. FTIR (ATR) υ (cm^{-1}): 3287 (NH), 3070 ($CH_{aromatic}$), 2922 ($CH_{aliphatic}$), 1679 (>C═O), 1651, 1594, 1560, 1501, 1461, 1374, 1311, 1274, 1197, 1130, 1064. ^{1}H NMR (500 MHz, *CDCl$_3$*) δ (ppm): 9.13–8.98 (m, 1H, $CH_{aromatic}$), 8.49–8.37 (m, 1H, $CH_{aromatic}$), 7.76–7.56 (m, 1H, $CH_{aromatic}$), 7.56–7.38 (m, 1H, NH), 7.22–6.94 (m, 2H, $CH_{aromatic}$), 6.94–6.78 (m, 1H, $CH_{aromatic}$), 2.44–2.14 (m, 6H, CH_3). ^{13}C NMR (125 MHz, *CDCl$_3$*) δ (ppm): 180.06, 175.77 (>C═O), 155.39, 148.44, 141.68, 135.72, 135.61, 134.73, 130.58, 130.13, 127.93, 126.81, 114.79 ($C_{aromatic}$ and C_q), 20.88, 17.77 (CH_3). HRMS(+ESI) *m/z* calcd for $C_{17}H_{14}^{35}ClN_2O_2$ [M + H]$^+$: 313.0744; found: 313.0724 and $C_{17}H_{14}^{37}ClN_2O_2$ [M + H]$^+$: 315.0714; found: 315.0726.

4.3.14. 7-Chloro-6-(3,4-dimethylphenyl)amino-5,8-quinolinequinone (AQQ14) [53]

By subjecting the mixture (**2** and $CeCl_3.7H_2O$) and 3,4-dimethylaniline (0.167 g, 1.375 mmol) to the general procedure for the synthesis of the **AQQ14**, the title compound (**AQQ14**) was purified by column chromatography as an orange solid. Yield: 23%, mp 194–195 °C. FTIR (ATR) υ (cm^{-1}): 3341 (NH), 3085 ($CH_{aromatic}$), 2978, 2919 ($CH_{aliphatic}$), 1669 (>C═O), 1605, 1575, 1507, 1311, 1293, 1222, 1145, 1064. ^{1}H NMR (500 MHz, DMSO-d_6) δ (ppm): 9.25 (s, 1H, $CH_{aromatic}$), 8.98 (s, 1H, $CH_{aromatic}$), 8.37 (d, 1H, $CH_{aromatic}$), 7.77–7.80 (m, 1H, $CH_{aromatic}$), 7.07 (d, J = 7.4 Hz, 1H, $CH_{aromatic}$), 6.94 (s, 1H, NH), 6.88 (d, J = 7.5 Hz, 1H, $CH_{aromatic}$), 2.50 (s, 3H, CH_3), 2.20 (s, 3H, CH_3). ^{13}C NMR (125 MHz, DMSO-d_6) δ (ppm): 180.45, 175.68 (>C═O), 154.86, 148.27, 143.28, 136.77, 136.13, 134.85, 133.13, 129.34, 127.96, 127.63, 125.68, 122.14, 115.14 ($C_{aromatic}$ and C_q), 19.90, 19.34 (CH_3). HRMS(+ESI) *m/z* calcd for $C_{17}H_{14}^{35}ClN_2O_2$ [M + H]$^+$: 313.0744; found: 313.0740 and $C_{17}H_{14}^{37}ClN_2O_2$ [M + H]$^+$: 315.0714; found: 315.0730.

4.3.15. 7-Chloro-6-(3,5-dimethylphenyl)amino-5,8-quinolinequinone (AQQ15)

By subjecting the mixture (**2** and $CeCl_3.7H_2O$) and 3,5-dimethylaniline (0.167 g, 1.375 mmol) to the general procedure for the synthesis of the **AQQ15**, the title compound (**AQQ15**) was purified by column chromatography as a brown solid. Yield: 72%, mp 224–226 °C. FTIR (ATR) υ (cm^{-1}): 3306 (NH), 3056 ($CH_{aromatic}$), 2911 ($CH_{aliphatic}$), 1677 (>C═O), 1654, 1586, 1559, 1510, 1424, 1297, 1265, 1202, 1141, 1067. ^{1}H NMR (500 MHz, *CDCl$_3$*) δ (ppm): 9.12–8.97 (m, 1H, $CH_{aromatic}$), 8.49–8.34 (m, 1H, $CH_{aromatic}$), 7.71–7.53 (m, 2H, NH and $CH_{aromatic}$), 6.92–6.80 (m, 1H, $CH_{aromatic}$), 6.77–6.61 (m, 2H, $CH_{aromatic}$), 2.34–2.27 (m, 6H, CH_3). ^{13}C NMR (125 MHz, *CDCl$_3$*) δ (ppm): 180.16, 175.88 (>C═O), 155.28, 148.37, 141.07, 138.25, 136.71, 134.77, 127.78, 126.85, 122.02, 115.82 ($C_{aromatic}$ and C_q), 21.28, 21.21 (CH_3). HRMS (+ESI) *m/z* calcd for $C_{17}H_{14}^{35}ClN_2O_2$ [M + H]$^+$: 313.0744; found: 313.0745 and $C_{17}H_{14}^{37}ClN_2O_2$ [M + H]$^+$: 315.0714; found: 315.0725.

4.3.16. 7-Chloro-6-(2-isopropylphenyl)amino-5,8-quinolinequinone (AQQ16)

By subjecting the mixture (**2** and $CeCl_3.7H_2O$) and 2-isopropylaniline (0.186 g, 1.375 mmol) to the general procedure for the synthesis of the **AQQ16**, the title compound (**AQQ16**) was purified by column chromatography as a red oil. Yield: 48%. FTIR (ATR) υ (cm^{-1}): 3318 (NH), 3067 ($CH_{aromatic}$), 2962, 2867 ($CH_{aliphatic}$), 1675 (>C═O), 1593, 1560, 1500, 1308, 1259, 1218, 1144, 1084, 1025. ^{1}H NMR (500 MHz, *CDCl$_3$*) δ (ppm): 9.06 (br s, 1H, $CH_{aromatic}$), 8.44 (s, 1H, $CH_{aromatic}$), 7.66 (s, 1H, $CH_{aromatic}$), 7.53 (s, 1H, NH), 7.33–7.26 (m, 2H, $CH_{aromatic}$), 7.18 (s, 1H, $CH_{aromatic}$), 7.03 (d, J = 7.0 Hz, 1H, $CH_{aromatic}$), 3.27–3.11 (m, 1H, CH), 1.26 (d, J = 5.4 Hz, 6H, CH_3). ^{13}C NMR (125 MHz, *CDCl$_3$*) δ (ppm): 180.03, 175.68 (>C═O), 155.30, 148.36, 143.94, 142.00, 134.85, 134.70, 127.73, 126.99, 126.85, 125.97, 125.60, 114.66 ($C_{aromatic}$ and C_q), 28.62 (CH), 22.92 (CH_3). MS (MALDI TOF) *m/z*: 327 [M+H]$^+$. Anal. Calcd. for $C_{18}H_{15}ClN_2O_2$ (326.08). HRMS(+ESI) *m/z* calcd for $C_{18}H_{16}^{35}ClN_2O_2$ [M + H]$^+$: 327.0900; found: 327.0898 and $C_{18}H_{16}^{37}ClN_2O_2$ [M + H]$^+$: 329.0871; found: 329.0888.

4.3.17. 7-Chloro-6-(3-isopropylphenyl)amino-5,8-quinolinequinone (AQQ17)

By subjecting the mixture (**2** and $CeCl_3.7H_2O$) and 3-isopropylaniline (0.186 g, 1.375 mmol) to the general procedure for the synthesis of the **AQQ17**, the title compound (**AQQ17**) was purified by column chromatography as a dark purple solid. Yield: 48%, mp 177–178 °C. FTIR (ATR) υ (cm^{-1}): 3303 (NH), 3056 ($CH_{aromatic}$), 2955, 2930 ($CH_{aliphatic}$), 1677 (>C═O), 1655, 1560, 1514, 1479, 1464, 1429, 1308, 1291, 1224, 1203, 1145, 1101, 1060. ^{1}H NMR (500 MHz, *CDCl$_3$*) δ (ppm): 9.15–9.01 (m, 1H, $CH_{aromatic}$), 8.52–8.39 (m, 1H, $CH_{aromatic}$), 7.85–7.56 (m, 2H, NH and $CH_{aromatic}$), 7.38–7.20 (m, 1H, $CH_{aromatic}$), 7.18–7.04 (m, 1H, $CH_{aromatic}$), 7.02–6.86 (m, 2H, $CH_{aromatic}$), 3.03–2.81 (m, 1H, CH), 1.34–1.19 (m, 6H, CH_3). ^{13}C NMR (125 MHz, *CDCl$_3$*) δ (ppm): 180.14, 175.79 (>C═O), 155.30, 149.46, 148.30, 140.97, 136.81, 134.92, 128.43, 126.94, 124.33, 122.60, 121.72, 115.66 ($C_{aromatic}$ and C_q), 33.93 (CH), 23.81 (CH_3). HRMS(+ESI) *m/z* calcd for $C_{18}H_{16}^{35}ClN_2O_2$ [M + H]$^+$: 327.0900; found: 327.0864 and $C_{18}H_{16}^{37}ClN_2O_2$ [M + H]$^+$: 329.0871; found: 329.0869.

4.3.18. 7-Chloro-6-(4-isopropylphenyl)amino-5,8-quinolinequinone (AQQ18)

By subjecting the mixture (**2** and $CeCl_3.7H_2O$) and 4-isopropylaniline (0.186 g, 1.375 mmol) to the general procedure for the synthesis of the **AQQ18**, the title compound (**AQQ18**) was purified by column

chromatography as a dark red solid. Yield: 12%, mp 160–161 °C. FTIR (ATR) υ (cm^{-1}): 3336 (NH), 3070 ($CH_{aromatic}$), 2957, 2870 ($CH_{aliphatic}$), 1672 (>C═O), 1606, 1577, 1520, 1497, 1463, 1312, 1281, 1217, 1144, 1066, 1019. ^{1}H NMR (500 MHz, *CDCl$_3$*) δ (ppm): 8.97 (dd, *J* = 4.7, 1.6 Hz, 1H, $CH_{aromatic}$), 8.35 (dd, *J* = 7.8, 1.7 Hz, 1H, $CH_{aromatic}$), 7.62 (s, 1H, NH), 7.57 (dd, *J* = 7.8, 4.7 Hz, 1H, $CH_{aromatic}$), 7.14 (d, *J* = 8.4 Hz, 2H, $CH_{aromatic}$), 6.95 (d, *J* = 8.4 Hz, 2H, $CH_{aromatic}$), 2.93–2.78 (m, 1H, CH), 1.19 (d, *J* = 6.9 Hz, 6H, CH_3). ^{13}C NMR (125 MHz, *CDCl$_3$*) δ (ppm): 180.15, 175.84 (>C═O), 155.37, 148.43, 147.07, 141.21, 134.85, 134.65, 126.91, 126.51, 124.45, 115.53 ($C_{aromatic}$ and C_q), 33.68 (CH), 23.97 (CH_3). MS (MALDI TOF) *m/z*: 326 $[M]^+$. Anal. Calcd. for $C_{18}H_{15}ClN_2O_2$ (326.08). HRMS(+ESI) *m/z* calcd for $C_{18}H_{16}^{35}ClN_2O_2$ $[M + H]^+$: 327.0900; found: 327.0900 and $C_{18}H_{16}^{37}ClN_2O_2$ $[M + H]^+$: 329.0871; found: 329.0885.

4.3.19. 7-Chloro-6-(4-(diethylamino)phenyl)amino-5,8-quinolinequinone (AQQ19)

By subjecting the mixture (**2** and $CeCl_3.7H_2O$) and *N,N*-diethyl-*p*-phenylenediamine (0.226 g, 1.375 mmol) to the general procedure for the synthesis of the **AQQ19**, the title compound (**AQQ19**) was purified by column chromatography as a dark green solid. Yield: 91%, mp 146–147 °C. FTIR (ATR) υ (cm^{-1}): 3315 (NH), 3052 ($CH_{aromatic}$), 2956 ($CH_{aliphatic}$), 1670 (>C═O), 1596, 1566, 1524, 1502, 1355, 1304, 1265, 1195. ^{1}H NMR (500 MHz, *CDCl$_3$*) δ (ppm): 9.06 (s, 1H, $CH_{aromatic}$), 8.43 (d, *J* = 6.8 Hz, 1H, $CH_{aromatic}$), 7.69 (s, 1H, $CH_{aromatic}$), 7.63 (br s, 1H, NH), 6.99–6.98 (m, 2H, $CH_{aromatic}$), 6.64–6.63 (m, 2H, $CH_{aromatic}$), 3.49–3.30 (m, 4H, NCH_2), 1.26–1.13 (m, 6H, NCH_2CH_3). ^{13}C NMR (125 MHz, *CDCl$_3$*) δ (ppm): 180.28, 175.59 (>C═O), 155.26, 148.73, 146.41, 141.23, 134.68, 126.82, 126.57, 126.21, 124.90, 110.99 ($C_{aromatic}$ and C_q), 44.47 (NCH_2), 12.54 (NCH_2CH_3). MS (MALDI TOF) *m/z*: 355 $[M]^+$. Anal. Calcd. for $C_{19}H_{18}ClN_3O_2$ (355.11). HRMS(+ESI) *m/z* calcd for $C_{19}H_{19}^{35}ClN_3O_2$ $[M + H]^+$: 356.1166; found: 356.1164 and $C_{19}H_{19}^{37}ClN_3O_2$ $[M + H]^+$: 358.1136; found: 358.1112.

4.4. Biochemistry

4.4.1. Cell culture and drug treatment

In the current study, HeLa cell line was cultured in Dulbecco's Modified Eagle Medium (DMEM) (Wako Pure Chemical Industries), while leukemia (K562, MT-2, and Jurkat) cell lines and PBMCs (Precision Bioservices, Frederic, MD) were cultured in RPMI 1640 (Wako Pure Chemical Industries) medium. Besides, 10% fetal bovine serum (FBS) (Sigma Aldrich, MO, USA) and 89 μg/mL streptomycin (Meiji Seika Pharma, Tokyo, Japan) were involved in DMEM and RPMI 1640 medium. All these cells were incubated at 37 °C in humidified 5% CO_2 atmosphere and implemented into 24-well (4×10^4 cells/mL) and 96-well (1×10^6 cells/mL) tissue plates (Iwaki brand Asahi Glass Co., Chiba, Japan) and then incubated again for 24 h (the optimum cell number was verified relevant to previous study) [73,74]. The stock solution of compounds **AQQ1-19** and imatinib in concentrations ranging from 0.1 to 10 mM were prepared in DMSO (Wako Pure Chemical Industries) and further diluted with fresh culture medium. The final DMSO concentration was left as 1% to hamper its any effect on the cell viability [75].

4.4.2. MTT assay

Based on the previously described procedures in literature [76,77], MTT (Dojindo Molecular Technologies, Kumamoto, Japan) assay was carried out with small modifications [78].

4.4.3. Detection of cell death

Apoptotic/necrotic/healthy/detection kit (PromoKine, Heidelberg, Germany) was administered with some modifications on manufacturer's directions [79,80], after K562 cell line was incubated with the most effective antiproliferative agents in this series at 1 μM concentration for 12 h. K562 cells, which were subject to proper content including binding buffer and staining solution, were analyzed by all-in-one fluorescence microscope Biorevo Fluorescence BZ-9000 (Keyence, Osaka, Japan). Based on our previous research [81], the number of healthy and necrotic cells was quantified related to the staining with annexin V and ethidium homodimer III.

4.4.4. Kinase inhibitory activity

Manufacturer's directions (Promega Corporation, Madison, WI, USA) were carried out with small amendments for the ABL1 kinase profiling assay application [82,83].

4.4.5. DNA cleavage activity

The DNA cleavage assay was applied associated with previously described method with some modification [84]. The most effective cytotoxic agents were investigated for determination of the DNA-cleaving activity by means of supercoiled pUC19 DNA and agarose (Takara, Kyoto, Japan) gel electrophoresis Mupid-2x (Mupid, Tokyo, Japan). Compounds were subject to pUC19 DNA (2 μg) in water and Tris/boric acid (Nacalai Tesque, Kyoto, Japan) buffer (10 mM, pH 8.5) with and without iron (II) sulfate heptahydrate ($FeSO_4.7H_2O$; 30 μM) (Wako Pure Chemical Industries), hydrogen peroxide (H_2O_2; 30 μM) (Tokyo Chemical Industry Co., Tokyo, Japan) and ascorbic acid (as an activator) (30 μM) (Tokyo Chemical Industry Co., Tokyo, Japan). The steps were followed in order: 1) incubation of the reaction mixture at 37 °C for 2 h, 2) addition of EDTA (Dojindo Molecular Technologies) and loading buffer (Takara, Kyoto, Japan), 3) application of agarose gel electrophoresis of pUC19 DNA at 100 V for 30 min in 1% slab gels carrying ethidium bromide (Wako Pure Chemical Industries) in Tris/-Boronic acid/EDTA buffer. Lastly, the fluorescence of intercalated ethidium bromide under a UV illuminator (Nippon Genetics Co., Tokyo, Japan) was photographed.

4.5. Molecular docking studies

Ligands were prepared in Maestro molecular modeling workspace followed by energy minimization in ligand preparation program of Schrödinger's Maestro molecular modeling package (Schrödinger Release 2016-2: Schrödinger, LLC, New York, NY, USA) under Optimized Potential Liquid Simulations (OPLS_2005) force field at physiological pH (pH = 7.4). The X-ray crystallographic structure of DNA was obtained from the PDB server (PDB entry: 1BNA) [62,63] and optimized for docking studies in protein preparation module of Schrödinger software. In molecular docking simulations: Grid Generation and Glide/XP docking protocols were applied (Schrödinger Release 2016-2: Schrödinger, LLC, New York, NY, USA) [85].

4.6. In silico absorption, distribution, metabolism, and excretion (ADME) prediction

Some ADME characteristics of the analogs **AQQ1-19** were screened by QikProp module of Schrödinger software (Schrödinger Release 2016-2: QikProp, Schrödinger, LLC, New York, NY, 2016) [85].

Author statement

The corresponding authors are responsible for ensuring that the descriptions are accurate and agreed by all authors.

Declaration of competing interest

The authors declare that they have no known competing financial interests or personal relationships that could have appeared to influence the work reported in this paper.

Acknowledgments

This work was financially supported by the Scientific and Technological Research Council of Turkey (TÜBİTAK), Grant No.: 118Z620 for supplying the equipment and materials. The authors thank both the Central Laboratory of the Middle-East Technical University and Advanced Technology Laboratory of the Kütahya Dumlupınar University for High-Resolution Mass Spectroscopy measurements for mass analyses. The crystallographic data have been deposited at the Cambridge Crystallographic Data Centre, and CCDC reference number are 2052461 for the **AQQ3**, 2052462 for the **AQQ7**, 2052463 for the **AQQ13**, and 2052464 for the **AQQ15**. The data can be obtained available free of charge from http://www.ccdc.cam.ac.uk/conts/retrieving.html or from the Cambridge Crystallographic Data Centre (CCDC), 12 Union Road, Cambridge CB2 1EZ, UK; fax: +44 (0)1223336033; email: deposit@ccdc.cam.ac.uk. We also thank Sadık Metin Ceyhan for helpful discussions on crystal structure analyses.

Appendix A. Supplementary data

Supplementary data to this article can be found online at https://doi.org/10.1016/j.cbi.2021.109555.

References

[1] G.M. Cragg, D.J. Newman, Plants as a source of anti-cancer and anti-HIV agents, Ann. Appl. Biol. 143 (2003) 127–133.
[2] D.J. Newman, G.M. Cragg, Natural products as sources of new drugs over the last 25 years, J. Nat. Prod. 70 (2007) 461–477.
[3] G.M. Cragg, P.G. Grothaus, D.J. Newman, Impact of natural products on developing new anti-cancer agents, Chem. Rev. 109 (2009) 3012–3043.
[4] D.J. Newman, G.M. Cragg, Natural products as sources of new drugs from 1981 to 2014, J. Nat. Prod. 79 (2016) 629–661.
[5] J. Sharifi-Rad, A. Ozleyen, T.B. Tumer, C.O. Adetunji, N. El Omari, A. Balahbib, Y. Taheri, A. Bouyahya, M. Martorell, N. Martins, W.C. Cho, Natural products and synthetic analogs as a source of antitumor drugs, Biomolecules 9 (2019) 679.
[6] F.E. Koehn, G.T. Carter, The evolving role of natural products in drug discovery, Nat. Rev. Drug Discov. 4 (2005) 206–220.
[7] J. Iqbal, B.A. Abbasi, T. Mahmood, S. Kanwal, B. Ali, S.A. Shah, A.T. Khalil, Plant-derived anticancer agents: a green anticancer approach, Asian Pac. J. Trop. Bio. 7 (2017) 1129–1150.
[8] K.V. Rao, W.P. Cullen, in: H. Welch, F. Marti-Ibanez (Eds.), Antibiotics Annual, 1959-1960, Medical Encyclopedia Inc, New York, 1960, pp. 950–953.
[9] S.G. Giorgi-Renault, J. Renault, M. Baron, P. Servolles, C. Paoletti, S. Cros, Heterocyclic quinones. VI: synthesis and antitumoral effects of 5,10-benzo[g]quinoxalinediones and aza-analogs, Eur. J. Med. Chem-Chim. Ther. 20 (1985) 144–148.
[10] Y. Yamashita, S. Kawada, N. Fujii, H. Nakano, Induction of mammalian DNA topoisomerase II dependent DNA cleavage by antitumor antibiotic streptonigrin, Can. Res. 50 (1990) 5841–5844.
[11] M. Levine, M. Borthwick, The action of streptonigrin on bacterial DNA metabolism and on induction of phage production in lysogenic bacteria, Virology 21 (1963) 568–574.
[12] M.A. Chirigos, J.W. Pearson, T.S. Papas, W.A. Woods, H.B. Wood Jr., G. Spahn, Effect of streptonigrin (NSC-45383) and analogs on oncornavirus replication and DNA polymerase activity, Cancer Chemother. Rep. 57 (1973) 305–309.
[13] Y. Inouye, Y. Take, S. Nakamura, H. Nakashima, N. Yamamoto, H. Kawaguchi, Screening for inhibitors of avian myeloblastosis virus reverse transcriptase and effect on the replication of AIDS-virus, J. Antibiot. (Tokyo) 40 (1987) 100–104.
[14] M. Kadela, M. Jastrzebska, E. Bebenek, E. Chrobak, M. Latocha, J. Kusz, M. Ksiazek, S. Boryczka, Synthesis, Structure and cytotoxic activity of mono- and dialkoxy derivatives of 5,8-quinolinedione, Molecules 21 (2016) 156.
[15] M.E. Suh, M.J. Kang, H.W. Yoo, S.Y. Park, C.O. Lee, Synthesis and cytotoxicity of 2-methyl-1-substituted-imidazo [4,5-g]quinoline-4,9-dione and 7,8-dihydro-10H-[1,4]oxazino[3',4':2,3]imidazo[4,5-g]quinoline-5,12-dio ne derivatives, Bioorg. Med. Chem. 8 (2000) 2079–2083.
[16] E.W. Humphrey, N. Blank, Clinical experience with streptonigrin, Cancer Chemother. Rep. 12 (1961) 99–103.
[17] M.E. Suh, S.Y. Park, C.O. Lee, Synthesis of pyridino[2,3-f]indole-4,9-dione and 6,7-disubstituted quinoline-5,8-dione derivatives and evaluation on their cytotoxic activity, Bioorg. Med. Chem. 9 (2001) 2979–2986.
[18] D.M. Balitz, J.A. Bush, W.T. Bradner, T.W. Doyle, F.A. O'Herron, D.E. Nettleton, Isolation of lavendamycin, a new antibiotic from Streptomyces lavendulae, J. Antibiot. (Tokyo) 35 (1982) 259–265.
[19] G. Bringmann, Y. Reichert, V.V. Kane, The total synthesis of streptonigrin and related antitumor antibiotic natural products, Tetrahedron 60 (2004) 3539–3574.
[20] A.J. Herlt, R.W. Rickards, J.P. Wu, The structure of streptonigrone, and a comment on the biosynthesis of the streptonigrin antibiotics, J. Antibiot. (Tokyo) 38 (1985) 516–518.
[21] Y. Fang, C.M. Linardic, D.A. Richardson, W. Cai, M. Behforouz, R.T. Abraham, Characterization of the cytotoxic activities of novel analogues of the antitumor agent, lavendamycin, Mol. Cancer Ther. 2 (2003) 517–526.
[22] M. Hassani, W. Cai, D.C. Holley, J.P. Lineswala, B.R. Maharjan, G.R. Ebrahimian, H. Seradj, M.G. Stocksdale, F. Mohammadi, C.C. Marvin, J.M. Gerdes, H.D. Beall, M. Behforouz, Novel lavendamycin analogues as antitumor agents: synthesis, in vitro cytotoxicity, structure-metabolism, and computational molecular modeling studies with NAD(P)H:quinone oxidoreductase 1, J. Med. Chem. 48 (2005) 7733–7749.
[23] W.B. Kremer, J. Laszlo, Comparison of biochemical effects of isopropylidine azastreptonigrin (NSC-62709) with streptonigrin (NSC-45383), Cancer Chemother. Rep. 51 (1967) 19–24.
[24] I.A. Shaikh, F. Johnson, A.P. Grollman, Streptonigrin 1. Structure-Activity-Relationships among simple bicyclic analogs - rate dependence of DNA-degradation on quinone reduction potential, J. Med. Chem. 29 (1986) 1329–1340.
[25] M. Behforouz, J. Haddad, W. Cai, Z.X. Gu, Chemistry of quinoline-5,8-diones, J. Org. Chem. 63 (1998) 343–346.
[26] M. Kimber, P.I. Anderberg, M.M. Harding, Synthesis of ABC analogues of the antitumour antibiotic streptonigrin, Tetrahedron 56 (2000) 3575–3581.
[27] S.J. Gould, S.M. Weinreb, Fortschr Streptonigrin, Chem. Org. Naturst. 41 (1982) 77–114.
[28] M.M. Harding, G.V. Long, Interaction of the antitumor antibiotic streptonigrin with metal ions and DNA, Curr. Med. Chem. 4 (1997) 405–420.
[29] H.A. Kontos, E.P. Wei, Hydroxyl radical-dependent inactivation of guanylate cyclase in cerebral arterioles by methylene blue and by LY83583, Stroke 24 (1993) 427–434.
[30] D. Lodygin, A. Menssen, H. Hermeking, Induction of the Cdk inhibitor p21 by LY83583 inhibits tumor cell proliferation in a p53-independent manner, J. Clin. Invest. 110 (2002) 1717–1727.
[31] K. Novak, Stopping the cycle, Nat. Rev. Canc. 3 (2003), 8-8.
[32] H.I. Ciftci, N. Bayrak, H. Yildirim, M. Yildiz, M.O. Radwan, M. Otsuka, M. Fujita, A. F. Tuyun, Discovery and structure-activity relationship of plastoquinone analogs as anticancer agents against chronic myelogenous leukemia cells, Arch. Pharm. 352 (1900170) (2019).
[33] N. Bayrak, H. Yildirim, M. Yildiz, M.O. Radwan, M. Otsuka, M. Fujita, A.F. Tuyun, H.I. Ciftci, Design, synthesis, and biological activity of Plastoquinone analogs as a new class of anticancer agents, Bioorg. Chem. 92 (103255) (2019).
[34] N. Bayrak, H. Yildirim, M. Yildiz, M.O. Radwan, M. Otsuka, M. Fujita, H.I. Ciftci, A. F. Tuyun, A novel series of chlorinated plastoquinone analogs: design, synthesis, and evaluation of anticancer activity, Chem. Biol. Drug Des. 95 (2020) 343–354.
[35] H. Yildirim, N. Bayrak, A.F. Tuyun, E.M. Kara, B.O. Celik, G.K. Gupta, 2,3-Disubstituted-1,4-naphthoquinones containing an arylamine with trifluoromethyl group: synthesis, biological evaluation, and computational study, RSC Adv. 7 (2017) 25753–25764.
[36] A.F. Tuyun, M. Yildiz, N. Bayrak, H. Yildirim, E.M. Kara, A.T. Jannuzzi, B.O. Celik, Discovery of a new family of heterocyclic amine linked plastoquinone analogs for antimicrobial evaluation, Drug Dev. Res. 80 (2019) 1098–1109.
[37] N. Bayrak, M. Yildiz, H. Yildirim, E.M. Kara, B.O. Celik, A.F. Tuyun, Brominated plastoquinone analogs: synthesis, structural characterization, and biological evaluation, J. Mol. Struct. 1219 (128560) (2020).
[38] E.M. Kara, N. Bayrak, H. Yildirim, M. Yildiz, B.O. Celik, A.F. Tuyun, Chlorinated plastoquinone analogs that inhibit Staphylococcus epidermidis and Candida albicans growth, Folia Microbiol. 65 (2020) 785–795.
[39] S. Keinan, W.D. Paquette, J.J. Skoko, D.N. Beratan, W. Yang, S. Shinde, P. A. Johnston, J.S. Lazo, P. Wipf, Computational design, synthesis and biological evaluation of para-quinone-based inhibitors for redox regulation of the dual-specificity phosphatase Cdc25B, Org. Biomol. Chem. 6 (2008) 3256–3263.
[40] C.K. Ryu, J.Y. Lee, S.H. Jeong, J.H. Nho, Synthesis and antifungal activity of 1H-pyrrolo[3,2-g]quinoline-4,9-diones and 4,9-dioxo-4,9-dihydro-1H-benzo[f]indoles, Bioorg, Med. Chem. Lett. 19 (2009) 146–148.
[41] A. Alfadhli, A. Mack, L. Harper, S. Berk, C. Ritchie, E. Barklis, Analysis of quinolinequinone reactivity, cytotoxicity, and anti-HIV-1 properties, Bioorg. Med. Chem. 24 (2016) 5618–5625.
[42] S.A. Egu, U.C. Okoro, E.A. Onoabedje, New aryl derivatives of quinolinedione and related heterocyclic compounds, J. Heterocycl. Chem. 54 (2017) 1572–1577.
[43] M. Kadela-Tomanek, M. Jastrzebska, E. Bebenek, E. Chrobak, M. Latocha, J. Kusz, D. Tarnawska, S. Boryczka, New acetylenic amine derivatives of 5,8-quinoline-diones: synthesis, crystal structure and antiproliferative activity, Crystals 7 (2017) 15.
[44] H. Yildirim, Arylthio analogs of 5,8-quinolinedione: synthesis, characterization, antibacterial, and antifungal evaluations, phosphorus sulfur silicon relat, Elements 195 (2020) 516–522.
[45] B.J. Mulchin, C.G. Newton, J.W. Baty, C.H. Grasso, W.J. Martin, M.C. Walton, E. M. Dangerfield, C.H. Plunkett, M.V. Berridge, J.L. Harper, M.S.M. Timmer, B. L. Stocker, The anti-cancer, anti-inflammatory and tuberculostatic activities of a series of 6,7-substituted-5,8-quinolinequinones, Bioorg. Med. Chem. 18 (2010) 3238–3251.
[46] L.L. Jing, G.C. Wu, X. Hao, F.A. Olotu, D.W. Kang, C.H. Chen, K.H. Lee, M.E. S. Soliman, X.Y. Liu, Y.N. Song, P. Zhan, Identification of highly potent and selective Cdc25 protein phosphatases inhibitors from miniaturization click-chemistry-based combinatorial libraries, Eur. J. Med. Chem. 183 (2019) 111696.
[47] K. Vazquez, C. Espinosa-Bustos, J. Soto-Delgado, R.A. Tapia, J. Varela, E. Birriel, R. Segura, J. Pizarro, H. Cerecetto, M. Gonzalez, M. Paulino, C.O. Salas, New

aryloxy-quinone derivatives as potential antiChagasic agents: synthesis, trypanosomicidal activity, electrochemical properties, pharmacophore elucidation and 3D-QSAR analysis, RSC Adv. 5 (2015) 65153–65166.
[48] A. Defant, I. Mancini, Design, synthesis and cancer cell growth inhibition evaluation of new aminoquinone hybrid molecules, Molecules 24 (2019) 2224.
[49] A. Defant, G. Guella, I. Mancini, Regioselectivity in the multi-component synthesis of indolizinoquinoline-5,12-dione derivatives, Eur. J. Org Chem. 2006 (2006) 4201–4210.
[50] E.Y. Yoon, H.Y. Choi, K.J. Shin, K.H. Yoo, D.Y. Chi, D.J. Kim, The regioselectivity in the reaction of 6,7-dihaloquinoline-5,8-diones with amine nucleophiles in various solvents, Tetrahedron Lett. 41 (2000) 7475–7480.
[51] M. Kadela-Tomanek, M. Jastrzebska, B. Pawelczak, E. Bebenek, E. Chrobak, M. Latocha, M. Ksiazek, J. Kusz, S. Boryczka, Alkynyloxy derivatives of 5,8-quinolinedione: synthesis, in vitro cytotoxicity studies and computational molecular modeling with NAD(P)H:Quinone oxidoreductase 1, Eur. J. Med. Chem. 126 (2017) 969–982.
[52] K.T. Santoso, A. Menorca, C.Y. Cheung, G.M. Cook, B.L. Stocker, M.S.M. Timmer, The synthesis and evaluation of quinolinequinones as anti-mycobacterial agents, Bioorg. Med. Chem. 27 (2019) 3532–3545.
[53] Y.S. Kim, S.Y. Park, H.J. Lee, M.E. Suh, D. Schollmeyer, C.O. Lee, Synthesis and cytotoxicity of 6,11-dihydro-pyrido- and 6,11-dihydro-benzo[2,3-b]phenazine-6,11-dione derivatives, Bioorg. Med. Chem. 11 (2003) 1709–1714.
[54] H.J. Lee, J.S. Kim, S.Y. Park, M.E. Suh, H.J. Kim, E.K. Seo, C.O. Lee, Synthesis and cytotoxicity evaluation of 6,11-dihydro-pyridazoand 6,11-dihydro-pyrido[2,3-blphenazine-6, 11-diones, Bioorg. Med. Chem. 12 (2004) 1623–1628.
[55] P. Jeschke, W. Lindner, N. Mueller, A. Harder, N. Mencke, in: A.-G. Bayer (Ed.), New 6(7)-Amino-Substituted-5,8-Quinolinediones to Combat Endoparasites, 1992, p. 37. Germany.
[56] S. Li, Src-family kinases in the development and therapy of Philadelphia chromosome-positive chronic myeloid leukemia and acute lymphoblastic leukemia, Leuk. Lymphoma 49 (2008) 19–26.
[57] J.R. Westin, R. Kurzrock, It's about time: lessons for solid tumors from chronic myelogenous leukemia therapy, Mol. Canc. Therapeut. 11 (2012) 2549–2555.
[58] P. Cohen, D. Cross, P.A. Janne, Kinase drug discovery 20 years after imatinib: progress and future directions, Nat. Rev. Drug Discov. (2021).
[59] R. Singh, A. Letai, K. Sarosiek, Regulation of apoptosis in health and disease: the balancing act of BCL-2 family proteins, Nat. Rev. Mol. Cell Biol. 20 (2019) 175–193.
[60] J.Y. Wang, Regulation of cell death by the Abl tyrosine kinase, Oncogene 19 (2000) 5643–5650.
[61] K. Samejima, W.C. Earnshaw, Trashing the genome: the role of nucleases during apoptosis, Nat. Rev. Mol. Cell Biol. 6 (2005) 677–688.
[62] L.M. Sousa, W.A. Souza, D.A. Paixao, R.B. Fazzi, D.Y. Tezuka, C.D. Lopes, Z. A. Carneiro, M.B. Moreira, M. Pivatto, A.V.G. Netto, S. de Albuquerque, F. B. Ferreira, R.J. De Oliveira, J.A.L.C. Resende, R.C. Lino, R.J. De Oliveira, A.M. D. Ferreira, W. Guerra, DNA binding, cleavage, apoptosis and cytotoxicity studies of three heteroleptic nickel complexes bearing beta-diketones, Inorg. Chim. Acta. 511 (119824) (2020).
[63] H.R. Drew, R.M. Wing, T. Takano, C. Broka, S. Tanaka, K. Itakura, R.E. Dickerson, Structure of a B-DNA dodecamer: conformation and dynamics, Proc. Natl. Acad. Sci. U.S.A. 78 (1981) 2179–2183.
[64] C.A. Lipinski, F. Lombardo, B.W. Dominy, P.J. Feeney, Experimental and computational approaches to estimate solubility and permeability in drug discovery and development settings, Adv. Drug Deliv. Rev. 46 (2001) 3–26.
[65] W.L. Jorgensen, E.M. Duffy, Prediction of drug solubility from structure, Adv. Drug Deliv. Rev. 54 (2002) 355–366.
[66] G. Capranico, M. Palumbo, S. Tinelli, F. Zunino, Unique sequence specificity of topoisomerase II DNA cleavage stimulation and DNA binding mode of streptonigrin, J. Biol. Chem. 269 (1994) 25004–25009.
[67] APEX2, Version 2014.1-1, Bruker AXS Inc., Bruker, 2014 (Madison, WI).
[68] SAINT, Version 8.34A, Bruker AXS Inc., Bruker, 2013. Madison, WI.
[69] SADABS, Version 2012/2, Bruker AXS Inc., Bruker, 2012. Madison, WI.
[70] SHELXTL, Version 6.14, Bruker AXS Inc., Bruker, 2000. Madison, WI.
[71] A.L. Spek, Structure validation in chemical crystallography, Acta Crystallogr. D 65 (2009) 148–155.
[72] C.F. Macrae, P.R. Edgington, P. McCabe, E. Pidcock, G.P. Shields, R. Taylor, M. Towler, J. van De Streek, Mercury: visualization and analysis of crystal structures, J. Appl. Crystallogr. 39 (2006) 453–457.
[73] T.F.S. Ali, H.I. Ciftci, M.O. Radwan, R. Koga, T. Ohsugi, Y. Okiyama, T. Honma, A. Nakata, A. Ito, M. Yoshida, M. Fujita, M. Otsuka, New SIRT2 inhibitors: histidine-based bleomycin spin-off, Bioorg. Med. Chem. 27 (2019) 1767–1775.
[74] E. Zeytun, M.D. Altintop, B. Sever, A. Ozdemir, D.E. Ellakwa, Z. Ocak, H.I. Ciftci, M. Otsuka, M. Fujita, M.O. Radwan, A new series of antileukemic agents: design, synthesis, in vitro and in silico evaluation of thiazole-based ABL1 kinase inhibitors, Anticancer Agents Med. Chem. (2020) 1099–1109.
[75] B. Sever, M.D. Altintop, A. Ozdemir, G. Akalin Ciftci, D.E. Ellakwa, H. Tateishi, M. O. Radwan, M.A.A. Ibrahim, M. Otsuka, M. Fujita, H.I. Ciftci, T.F.S. Ali, In vitro and in silico evaluation of anticancer activity of new indole-based 1,3,4-oxadiazoles as EGFR and COX-2 inhibitors, Molecules 25 (2020) 5190.
[76] M.O. Radwan, H.I. Ciftci, T.F.S. Ali, D.E. Ellakwa, R. Koga, H. Tateishi, A. Nakata, A. Ito, M. Yoshida, Y. Okamoto, M. Fujita, M. Otsuka, Antiproliferative S-Trityl-l-Cysteine -derived compounds as SIRT2 inhibitors: repurposing and solubility enhancement, Molecules 24 (2019) 3295.
[77] H.I. Ciftci, M. Can, D.E. Ellakwa, S.C. Suner, M.A. Ibrahim, A. Oral, N. Sekeroglu, B. Ozalp, M. Otsuka, M. Fujita, M. Alparslan, M.O. Radwan, Anticancer activity of Turkish marine extracts: a purple sponge extract induces apoptosis with multitarget kinase inhibition activity, Invest. N. Drugs 38 (2020) 1326–1333.
[78] M.O. Radwan, H.I. Ciftci, T.F.S. Ali, R. Koga, H. Tateishi, A. Nakata, A. Ito, M. Yoshida, M. Fujita, M. Otsuka, Structure activity study of S-trityl-cysteamine dimethylaminopyridine derivatives as SIRT2 inhibitors: improvement of SIRT2 binding and inhibition, Bioorg. Med. Chem. Lett 30 (2020) 127458.
[79] W. Shida, H. Tateishi, Y. Tahara, M. Fujita, D. Husham Majeed Alsaadi, M. Watanabe, R. Koga, M.O. Radwan, H.I. Ciftci, S. Gezici, Y. Kurauchi, H. Katsuki, M. Otsuka, K. Sugimura, M. Wada, N. Sekeroglu, T. Watanabe, Antileukemic activity of twig components of caucasian beech in Turkey, Molecules 24 (2019) 3850.
[80] H.I. Ciftci, Antiproliferative activity of α-tomatine and molecular target identification, Turk. J. Agri. Nat. Sci. 70 (2020) 290–300.
[81] H. Tateishi, K. Monde, K. Anraku, R. Koga, Y. Hayashi, H.I. Ciftci, H. DeMirci, T. Higashi, K. Motoyama, H. Arima, M. Otsuka, M. Fujita, A clue to unprecedented strategy to HIV eradication: "Lock-in and apoptosis, Sci. Rep. 7 (2017) 8957.
[82] H.I. Ciftci, M.O. Radwan, S.E. Ozturk, N.G. Ulusoy, E. Sozer, D.E. Ellakwa, Z. Ocak, M. Can, T.F.S. Ali, H.I. Abd-Alla, N. Yayli, H. Tateishi, M. Otsuka, M. Fujita, Design, synthesis and biological evaluation of pentacyclic triterpene derivatives: optimization of anti-ABL kinase activity, Molecules 24 (2019) 3535.
[83] H. Ciftci, Effects of glycyrrhetic acid on human chronic myelogenous leukemia cells, Turk. J. Pharm. Sci. 17 (2020) 49–55.
[84] T.F.S. Ali, K. Iwamaru, H.I. Ciftci, R. Koga, M. Matsumoto, Y. Oba, H. Kurosaki, M. Fujita, Y. Okamoto, K. Umezawa, M. Nakao, T. Hide, K. Makino, J. Kuratsu, M. Abdel-Aziz, G.E.D.A.A. Abuo-Rahma, E.A.M. Beshr, M. Otsuka, Novel metal chelating molecules with anticancer activity. Striking effect of the imidazole substitution of the histidine-pyridine-histidine system, Bioorg. Med. Chem. 23 (2015) 5476–5482.
[85] B. Sever, M.D. Altıntop, Y. Demir, M. Pekdoğan, G. Akalın Çiftçi, Ş. Beydemir, A. Özdemir, An extensive research on aldose reductase inhibitory effects of new 4H-1,2,4-triazole derivatives, J. Mol. Struct. 1224 (2021) 129446.